

# Diffusion with resetting in a logarithmic potential

Somrita Ray<sup>1, a)</sup> and Shlomi Reuveni<sup>1, b)</sup>

*School of Chemistry, The Center for Physics and Chemistry of Living Systems, The Raymond and Beverly Sackler Center for Computational Molecular and Materials Science, & The Ratner Center for Single Molecule Science, Tel Aviv University, Tel Aviv 69978, Israel*

(Dated: 26 March 2025)

We study the effect of resetting on diffusion in a logarithmic potential. In this model, a particle diffusing in a potential  $U(x) = U_0 \log|x|$  is reset, i.e., taken back to its initial position, with a constant rate  $r$ . We show that this analytically tractable model system exhibits a series of phase transitions as a function of a single parameter,  $\beta U_0$ , the ratio of the strength of the potential to the thermal energy. For  $\beta U_0 < -1$  the potential is strongly repulsive, preventing the particle from reaching the origin. Resetting then generates a non-equilibrium steady state which is characterized exactly and thoroughly analyzed. In contrast, for  $\beta U_0 > -1$  the potential is either weakly repulsive or attractive and the diffusing particle eventually reaches the origin. In this case, we provide a closed form expression for the subsequent first-passage time distribution and show that a resetting transition occurs at  $\beta U_0 = 5$ . Namely, we find that resetting can expedite arrival to the origin when  $-1 < \beta U_0 < 5$ , but not when  $\beta U_0 > 5$ . The results presented herein generalize results for simple diffusion with resetting — a widely applicable model that is obtained from ours by setting  $U_0 = 0$ . Extending to general potential strengths, our work opens the door to theoretical and experimental investigation of a plethora of problems that bring together resetting and diffusion in logarithmic potential.

## I. INTRODUCTION

Resetting, i.e., stopping an ongoing dynamical process to start it anew, has recently gained significant attention due to its prevalence in natural and man made systems. For example, it has long been known that resetting certain computer algorithms can significantly enhance their performance<sup>1–4</sup>. Resetting is also commonly considered in the context of search processes<sup>5–14</sup>, e.g., foraging animals and birds come back to their dens and nests repeatedly<sup>15,16</sup>; and inconvenient weather may force a team of rescuers to temporarily stop their search efforts and return to base<sup>10</sup>. Natural disasters and epidemics may also lead to resetting, e.g., by drastically reducing the population of a living species in a certain locality<sup>17</sup>; and stock market crashes have a similar effect on asset prices<sup>18</sup>. At the microscopic level, resetting is an integral part of the well-known Michaelis-Menten reaction scheme of enzymatic catalysis<sup>19–22</sup>. This scheme is used to describe a variety of cellular processes<sup>23</sup> ranging from RNA transcription<sup>24</sup> to facilitated diffusion<sup>25,26</sup> and from the work of GTPase proteins<sup>27</sup> to chaperone assisted protein folding<sup>28</sup>. For all these reasons and others, resetting and its applications have now become a focal point of scientific interest<sup>29</sup>.

Diffusion with stochastic resetting serves as a paradigmatic model to understand resetting phenomena<sup>30–41</sup>. In this model, one considers a Brownian particle that returns to its initial position randomly in time. This resetting process drives the system away from equilibrium, giving rise to a nonequilibrium steady state and interesting relaxation dynamics. In the presence of an absorbing boundary, this model also provides a classical example of a system where resetting accelerates the completion of a first-passage process<sup>43,44</sup>.

In many cases, diffusion occurs in the presence of a bias. A natural way to model such phenomena is to consider a Brownian particle in a suitable potential landscape. Similar to free-diffusion, resetting then leads to a nonequilibrium steady state<sup>45</sup>. The scenario gets more interesting in the presence of an absorbing boundary since resetting then plays a dual role: either facilitating or hindering the resulting first-passage process<sup>10</sup>. Moreover, as system parameters are varied, resetting can invert its role thereby leading to a resetting transition<sup>5,19,20,46</sup>. This transition, as well as the emergence of non-equilibrium steady states, were recently explored for diffusion in various potential landscapes, e.g., linear, harmonic and power-law<sup>45–50</sup>. An important potential landscape that was not considered despite its centrality is the logarithmic potential.

The logarithmic potential arises as an effective potential in a large variety of problems in statistical and biological physics. For example, in the denaturation process of double-stranded DNA, it appears as an entropic term in the free energy cost of unzipping DNA base-pairs that generate denaturation bubbles<sup>51–56</sup>. Diffusion in an effective logarithmic potential is a popular model to study the spreading of momenta of cold atoms trapped in optical lattices<sup>57–64</sup>. The interactions of colloids and polymers with walls of narrow channels and pores give rise to an “entropic” potential that is logarithmic<sup>65–71</sup>. Log potential also arises in Dyson’s Brownian motion, where Coulomb gas is interpreted as a dynamical system to explore the eigenvalues of random matrices<sup>72,73</sup>. Other well-known examples include systems with long-range interacting particles<sup>74</sup>, self-gravitating Brownian particles<sup>75,76</sup>, charges in the vicinity of a polyelectrolyte<sup>77,78</sup> and interacting tracers in one-dimensional driven lattice gases<sup>79</sup>.

The logarithmic potential owns a central singularity at the origin, but behaves as a slowly varying function far away from it. Because of these unique features, diffusion in logarithmic potential leads to slow relaxation<sup>59,60,80,81</sup> and non-trivial first-passage properties<sup>82–84</sup>. A Brownian particle in a loga-

<sup>a)</sup>Electronic mail: somritaray@mail.tau.ac.il

<sup>b)</sup>Electronic mail: shlomire@tauex.tau.ac.il

rithmic potential is therefore expected to serve as an interesting model to study the effects of resetting on stochastic dynamics.

In strongly repulsive logarithmic potential, a diffusing particle cannot reach the origin<sup>82</sup>. Stochastic resetting is then expected to lead to a non-equilibrium steady state. In stark contrast, when the logarithmic potential is either attractive or weakly repulsive, a diffusing particle will reach the origin in finite time<sup>82</sup>. Stochastic resetting can then either accelerate or delay the resulting first passage process. Going from the strongly repulsive case to the attractive case can be done by tuning a single model parameter — the strength of the potential in units of the thermal energy. Diffusion with resetting in a logarithmic potential thus lends itself as attractive model to study stochastic resetting and the range response to it. In what follows, we provide a detailed analysis of this model system.

The rest of this paper is organized as follows. We start in Sec. II where we revisit some earlier works and review the problem of diffusion in a logarithmic potential. In Sec. III, we explore the properties of the nonequilibrium steady state that the particle attains due to resetting while it diffuses in a strongly repulsive logarithmic potential. Considering the potential to be attractive/weakly repulsive, in Sec. IV we study the first-passage of the particle in the presence of resetting to an absorbing boundary placed at the origin. In the same section, we also explore the resetting transition. The final conclusions are drawn in Sec. V, where we construct a full phase diagram for the present problem as a function of  $\beta U_0$  — the ratio of the strength of the logarithmic potential to the thermal energy.

## II. DIFFUSION IN A LOGARITHMIC POTENTIAL

Diffusion in a logarithmic potential has attracted considerable attention in recent years<sup>57–62,80–84</sup>. Here, we present a brief review of the problem. Consider a particle undergoing diffusion in a potential  $U(x) = U_0 \log|x|$  with constant strength  $U_0$ . The potential is attractive for  $U_0 > 0$  while it is repulsive for  $U_0 < 0$ . The diffusion constant  $D$  is given by the Einstein-Smoluchowski relation  $D = (\beta \zeta)^{-1}$ , where  $\beta$  is the thermodynamic *beta* and  $\zeta$  stands for the friction coefficient. An absorbing boundary is placed at the origin such that the particle, starting from a position  $x_0 > 0$ , diffuses in the interval  $0 < x < \infty$  until it hits the origin and is immediately removed from the system.

The time evolution of  $p(x, t)$ , the conditional probability density of finding the particle at position  $x$  at time  $t$  provided that the initial position was  $x_0$ , is then given by the Fokker-Planck equation

$$\frac{\partial p(x, t)}{\partial t} = \frac{\partial}{\partial x} \left[ \left( \frac{U_0}{\zeta x} \right) p(x, t) \right] + D \frac{\partial^2 p(x, t)}{\partial x^2}, \quad (1)$$

where the initial condition is  $p(x, 0) = \delta(x - x_0)$  and the boundary condition reads  $p(0, t) = 0$ . Eq. (1) is exactly solvable<sup>82</sup>. To present the solution, first we define the param-

eter

$$\nu := \frac{1 + \beta U_0}{2}. \quad (2)$$

The solution to Eq. (1) then reads<sup>82,84</sup>,

$$p(x, t) = \begin{cases} \frac{x}{2Dt} \left( \frac{x_0}{x} \right)^\nu \exp\left(-\frac{x^2 + x_0^2}{4Dt}\right) I_{-\nu}\left(\frac{xx_0}{2Dt}\right) & \text{if } \beta U_0 < -1, \\ \frac{x}{2Dt} \left( \frac{x_0}{x} \right)^\nu \exp\left(-\frac{x^2 + x_0^2}{4Dt}\right) I_\nu\left(\frac{xx_0}{2Dt}\right) & \text{if } \beta U_0 \geq -1, \end{cases} \quad (3)$$

where  $I_{\pm\nu}(\cdot)$  is the modified Bessel function of the first kind with order  $\pm\nu$ .

For  $\beta U_0 < -1$ , the potential is strongly repulsive. One then finds from Eq. (3) that  $p(x, t)$  is always normalized, i.e.,  $\int_0^\infty p(x, t) dx = 1$ . Therefore, in this case, the particle never reaches the absorbing boundary at the origin. In stark contrast, for  $\beta U_0 > -1$ , where the potential is either weakly repulsive or attractive, the particle eventually hits the absorbing boundary for every single realization. The survival probability  $Q(t) := \int_0^\infty p(x, t) dx$ , i.e., the probability that the particle is not absorbed at the origin by time  $t$ , is then given by<sup>84</sup>

$$Q(t) = 1 - \frac{\Gamma\left(\nu, \frac{x_0^2}{4Dt}\right)}{\Gamma(\nu)}, \quad (4)$$

where  $\Gamma(\nu) := \int_0^\infty x^{\nu-1} e^{-x} dx$  and  $\Gamma(\nu, a) := \int_a^\infty x^{\nu-1} e^{-x} dx$  denote the Gamma function and the upper incomplete Gamma function, respectively. The probability density function for the first-passage time (FPT) distribution to the origin can be calculated from the survival probability as  $f_T(t) = -\partial Q(t)/\partial t$ , which gives<sup>82,84</sup>

$$f_T(t) = \frac{t^{-(\nu+1)}}{\Gamma(\nu)} \left( \frac{x_0^2}{4D} \right)^\nu \exp\left(-\frac{x_0^2}{4Dt}\right). \quad (5)$$

Note that in the long time limit  $f_T(t) \propto t^{-(\nu+1)}$ . Consequently in the same limit  $Q(t) \propto t^{-\nu}$ . Thus  $\nu$  is known as the “persistence exponent”<sup>44</sup>, governing the decay of the survival probability. For free diffusion  $U_0 = 0$ , and Eq. (2) gives  $\nu = 1/2$ . Eq. (5) then reduces to the well-known form  $f_T(t) = \frac{x_0}{\sqrt{4\pi Dt^3}} \exp\left[-\frac{x_0^2}{4Dt}\right]$ , which describes the FPT of a freely diffusing particle to an absorbing boundary<sup>85</sup>.

The fact that the system behaves differently depending on the potential makes the current problem a highly interesting one to study the effect of stochastic resetting. On one hand, when the particle starting at  $x_0 > 0$  diffuses in a strongly repulsive logarithmic potential ( $\beta U_0 < -1$ ), its survival probability in the interval  $[0, \infty]$  does not decay with time. Introduction of stochastic resetting is then expected to lead to a non-equilibrium steady state. On the other hand, when the particle diffuses in either attractive or weakly repulsive logarithmic potential ( $\beta U_0 > -1$ ), its survival probability decays with time. Starting from  $x_0 > 0$ , it now takes finite time to reach the absorbing boundary placed at the origin. Introduction of resetting can then either expedite or delay completion

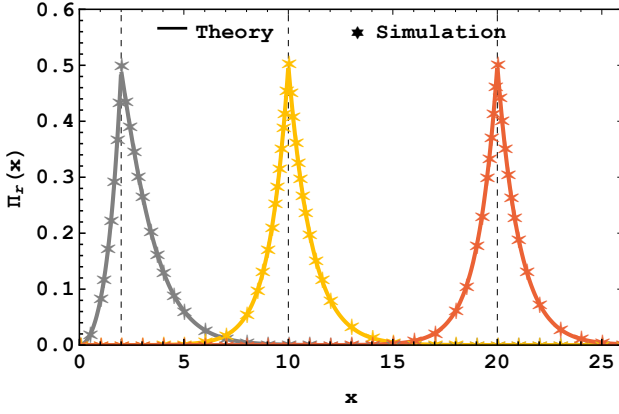


FIG. 1. The steady state distribution for diffusion in a strongly repulsive logarithmic potential under stochastic resetting. The theoretically predicted density  $\Pi_r(x)$  from Eq. (10) is plotted for different values of the initial position  $x_0 = \{2, 10, 20\}$ . The symbols showing simulation data are in excellent agreement with the theory. Here we have taken  $\beta U_0 = -2.0$  and  $\alpha_0 = 1.0$ .

of this first-passage process<sup>10</sup>. Motivated by these different possible outcomes, we study the effects of stochastic resetting on diffusion in a logarithmic potential.

### III. STEADY STATE WITH RESETTING

In this Section, we explore the effect of stochastic resetting on a particle diffusing in a strongly repulsive logarithmic potential, i.e., when  $\beta U_0 < -1$ . We assume that the particle is reset, i.e., taken back to its initial position  $x_0$ , with a constant rate  $r$ . This means that the times between two consecutive resetting events are taken from an exponential distribution with mean  $1/r$ . Setting  $p_r(x, t)$  as the conditional probability density of finding the particle at position  $x$  at time  $t$  provided that the initial position was  $x_0$ , the Fokker-Planck equation for the process with resetting reads

$$\frac{\partial p_r(x, t)}{\partial t} = \frac{\partial}{\partial x} \left[ \left( \frac{U_0}{\zeta x} \right) p_r(x, t) \right] + D \frac{\partial^2 p_r(x, t)}{\partial x^2} - r p_r(x, t) + r \delta(x - x_0), \quad (6)$$

where  $\delta(x - x_0)$  is a Dirac delta function. Note that in the absence of resetting ( $r = 0$ ), Eq. (6) boils down to Eq. (1), the Fokker-Planck equation for the underlying process. For  $r > 0$ , there is a loss of probability from position  $x$  and a gain of probability at position  $x_0$  due to resetting. The last two terms on the right hand side of Eq. (6) account for this additional probability flow, which is proportional to  $r$ , the resetting rate.

In what follows, we will be primarily interested in the steady state probability density of the process under stochastic resetting,  $\Pi_r(x) := \lim_{t \rightarrow \infty} p_r(x, t)$ . In the long time limit,

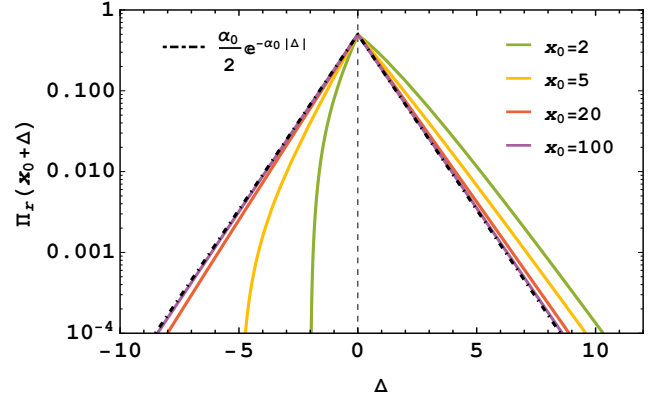


FIG. 2. The shifted steady state distribution  $\Pi_r(x_0 + \Delta)$  for different values of  $x_0$ , where  $\Delta \in \{-x_0, \infty\}$ . The solid lines are plotted using Eq. (10). The dot-dashed black line shows the asymptotic result of Eq. (11). Here we have taken  $\beta U_0 = -4.0$  and  $\alpha_0 = 1.0$ .

$\partial p_r(x, t)/\partial t = 0$ , and hence Eq. (6) gives

$$\frac{d^2 \Pi_r(x)}{dx^2} + \frac{d}{dx} \left[ \left( \frac{\beta U_0}{x} \right) \Pi_r(x) \right] - \left( \frac{r}{D} \right) \Pi_r(x) = - \left( \frac{r}{D} \right) \delta(x - x_0). \quad (7)$$

The conventional way to calculate  $\Pi_r(x)$  is to solve Eq. (7). We discuss this in detail in Appendix A. The same result can also be obtained using a general relation that connects the propagator of an underlying stochastic process  $p(x, t)$  with its steady state distribution under resetting,  $\Pi_r(x)$ . This relation is given by<sup>29</sup>

$$\Pi_r(x) = \int_0^\infty r e^{-rt} p(x, t) dt = r \tilde{p}(x, r), \quad (8)$$

where  $\tilde{p}(x, s) := \int_0^\infty e^{-st} p(x, t) dt$  denotes the Laplace transform of  $p(x, t)$ .

Therefore, in order to calculate  $\Pi_r(x)$ , we Laplace transform Eq. (3) for  $\beta U_0 < -1$  and set  $s = r$  to obtain [Appendix B]

$$\tilde{p}(x, r) = \begin{cases} \frac{x}{D} \left( \frac{x_0}{x} \right)^\nu I_{-\nu} \left( \sqrt{\frac{rx_0^2}{D}} \right) K_{-\nu} \left( \sqrt{\frac{rx^2}{D}} \right) & \text{if } x \geq x_0, \\ \frac{x}{D} \left( \frac{x_0}{x} \right)^\nu K_{-\nu} \left( \sqrt{\frac{rx_0^2}{D}} \right) I_{-\nu} \left( \sqrt{\frac{rx^2}{D}} \right) & \text{if } x < x_0. \end{cases} \quad (9)$$

Plugging in Eq. (9) into Eq. (8) and setting  $\alpha_0 := \sqrt{r/D}$ , we get the steady state density

$$\Pi_r(x) = \begin{cases} \alpha_0^2 x \left( \frac{x_0}{x} \right)^\nu I_{-\nu}(\alpha_0 x_0) K_{-\nu}(\alpha_0 x) & \text{if } x \geq x_0, \\ \alpha_0^2 x \left( \frac{x_0}{x} \right)^\nu K_{-\nu}(\alpha_0 x_0) I_{-\nu}(\alpha_0 x) & \text{if } x < x_0. \end{cases} \quad (10)$$

In Fig. 1, we plot  $\Pi_r(x)$  for different values of the initial position  $x_0$ . The solid lines denote the analytical results, obtained by plotting Eq. (10) and the symbols are coming from

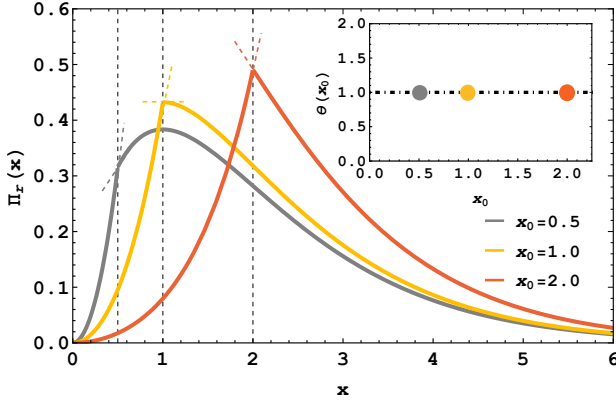


FIG. 3. Main: The steady state density  $\Pi_r(x)$  for different values of the initial position  $x_0$ .  $\Pi_r(x)$  has a cusp at  $x_0$  that coincides with its mode for moderate to high values of  $x_0$ . For small values of  $x_0$ , the mode of the distribution appears to the right of the cusp. Inset: The discontinuity in  $\partial\Pi_r(x)/\partial x$  at  $x = x_0$ , denoted  $\theta(x_0)$  [Eq. (13)], is a non-zero constant,  $\alpha_0^2$ . Here we have taken  $\beta U_0 = -2.0$  and  $\alpha_0 = 1$ .

Langevin dynamics simulation. The details of the numerical simulations are given in Appendix C.

Examining Fig. 1, we see that  $\Pi_r(x)$  is asymmetric for small values of  $x_0$ . The potential, being most repulsive at  $x = 0$ , pushes the particle away from the origin thereby generating this asymmetry. The effect dies down for higher values of  $x_0$ , resulting in a steady state density that is almost symmetric. Indeed, when  $x_0 \gg \alpha_0^{-1}$ , the particle is most likely to stay away from the origin, where the logarithmic potential varies slowly and is almost flat. This situation is similar to free diffusion. Therefore, in this limit  $\Pi_r(x)$  is expected to closely resemble a Laplace distribution, which describes the steady state density for free diffusion with stochastic resetting<sup>30</sup>.

In order to explore this further, we set  $x = x_0 + \Delta$  such that  $|\Delta|/x_0 \ll 1$ , and perform an asymptotic analysis of Eq. (10) in the limit  $x_0 \gg \alpha_0^{-1}$ . The limiting expressions of the modified Bessel functions for large arguments are  $\lim_{y \rightarrow \infty} I_{-\nu}(y) \simeq e^y/\sqrt{2\pi y}$  and  $\lim_{y \rightarrow \infty} K_{-\nu}(y) \simeq e^{-y}\sqrt{\pi/2y}$ , respectively<sup>87</sup>. Utilizing these together with Eq. (10) we get

$$\begin{aligned} \Pi_r(x) &= \Pi_r(x_0 + \Delta) \\ &\simeq_{x_0 \gg \alpha_0^{-1}} \frac{\alpha_0}{2} e^{-\alpha_0|\Delta|} \left( \frac{x_0}{x_0 + \Delta} \right)^{\nu-1} \frac{x_0}{\sqrt{x_0(x_0 + \Delta)}}, \\ &\simeq \frac{\alpha_0}{2} e^{-\alpha_0|x-x_0|}, \end{aligned} \quad (11)$$

where we have neglected all terms of order  $|\Delta|/x_0 \ll 1$ . Eq. (11) proves that when  $x_0 \gg \alpha_0^{-1}$ , the steady state distribution under resetting for diffusion in a logarithmic potential converges to a Laplace distribution. In Fig. 2, we plot the shifted steady state density  $\Pi_r(x_0 + \Delta)$  vs.  $\Delta$  to explicitly show that it merges with that of free diffusion<sup>30</sup> for sufficiently high values of  $x_0$ .

It is apparent from Fig. 1 and 2 that the steady state density has a cusp at the resetting position  $x_0$ . In what follows, we explore the cusp and the mode of the distribution in detail. In Fig. 3, we plot  $\Pi_r(x)$  for some moderate values of  $x_0$ ,

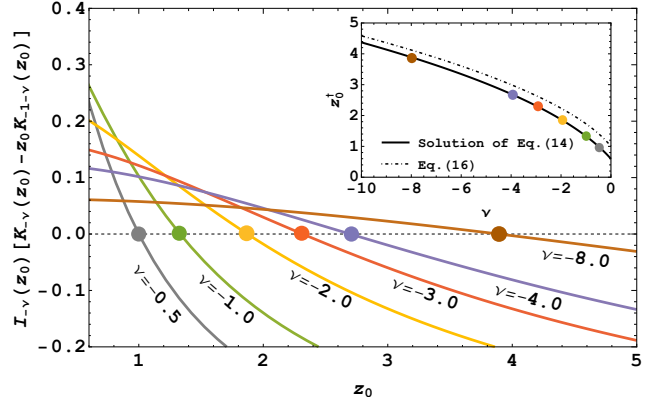


FIG. 4. Main: Graphical solution of Eq. (14) for different values of  $\nu$ . The solutions,  $z_0^\dagger$ , are highlighted by circles. Inset: Solid line shows the variation of  $z_0^\dagger$  vs.  $\nu$ , with colored circles corresponding to the values of  $\nu$  from the main figure. The dashed line shows the upper bound from Eq. (16).

highlighting the slopes from both sides of the cusp. Letting  $\Pi_r^-(x)$  and  $\Pi_r^+(x)$  denote the left and right branches of  $\Pi_r(x)$ , we obtain explicit expressions for these slopes

$$\begin{aligned} \left. \frac{\partial \Pi_r^+(x)}{\partial x} \right|_{x_0} &= \alpha_0^2 I_{-\nu}(\alpha_0 x_0) [K_{-\nu}(\alpha_0 x_0) - \alpha_0 x_0 K_{-1-\nu}(\alpha_0 x_0)], \\ \left. \frac{\partial \Pi_r^-(x)}{\partial x} \right|_{x_0} &= \alpha_0^2 K_{-\nu}(\alpha_0 x_0) [I_{-\nu}(\alpha_0 x_0) + \alpha_0 x_0 I_{-1-\nu}(\alpha_0 x_0)]. \end{aligned} \quad (12)$$

The difference between the slopes at  $x_0$  in Eq. (12) then reads

$$\theta(x_0) = \left[ \frac{\partial \Pi_r^-(x)}{\partial x} - \frac{\partial \Pi_r^+(x)}{\partial x} \right]_{x \rightarrow x_0} = \alpha_0^2, \quad (13)$$

where we utilized the identity<sup>87</sup>  $K_{-\nu}(y)I_{-1-\nu}(y) + I_{-\nu}(y)K_{-1-\nu}(y) = 1/y$ . Thus, regardless of the particle's initial position, the difference between the slopes at  $x_0$  is always  $\alpha_0^2$ , as is illustrated in the inset of Fig. 3. This non-zero difference proves that  $\Pi_r(x)$  always has a cusp at  $x_0$ . Note that Eq. (13) follows directly from Eq. (7), as we show in Appendix A.

It is evident from Fig. 3 that for moderate to high values of  $x_0$ , the mode of the distribution coincides with the cusp, whereas for small values of  $x_0$ , the mode appears to the right of the cusp. This effect arises due to the interplay between resetting and the action of the logarithmic potential. On one hand, resetting takes the particle back to  $x_0$  and thus increases the probability density of finding it there. On the other hand, the strongly repulsive potential pushes the particle away from the origin, thereby decreasing the probability density of finding it close to  $x = 0$ . For moderate to high values of  $x_0$ , the effect of resetting dominates: the cusp and the mode of  $\Pi_r(x)$  coincide. In contrast, for small values of  $x_0$  repulsion plays a significant role pushing the mode of the distribution to the right of the cusp.

In what follows, we will be interested in finding the

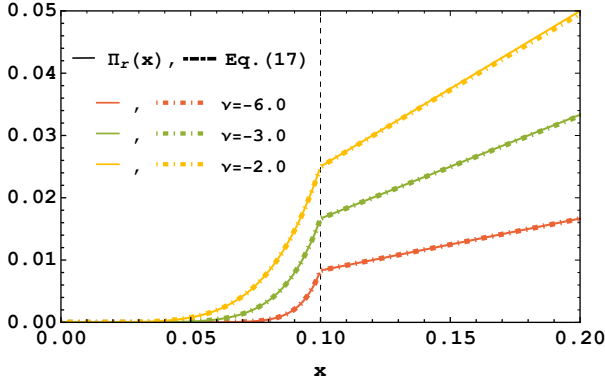


FIG. 5. The steady state distribution for different values of  $\nu$  in the limit  $x_0 \ll \alpha_0^{-1}$ . The solid lines denote  $\Pi_r(x)$  from Eq. (10). The dash-dotted lines show limiting results from Eq. (17). Here we have taken  $x_0 = 0.1$  and  $\alpha_0 = 1.0$ .

minimal value of  $x_0$ , denoted  $x_0^\dagger$ , for which the cusp and the mode of  $\Pi_r(x)$  coincide. To do that, we see from Fig. 3 that while the slope of  $\Pi_r^-(x)$  is always positive at  $x_0$ , that of  $\Pi_r^+(x)$  changes its sign. This transition happens at  $x_0^\dagger$ , where the slope of  $\Pi_r^+(x)$  is exactly zero. Setting  $\partial \Pi_r^+(x)/\partial x = 0$  and utilizing Eq. (12) gives the following transcendental equation

$$I_{-\nu}(z_0)[K_{-\nu}(z_0) - z_0 K_{-1-\nu}(z_0)] = 0, \quad (14)$$

where  $z_0 := \alpha_0 x_0$ . The solution to Eq. (14), denoted  $z_0^\dagger$ , can then be used to calculate the transition point

$$x_0^\dagger = z_0^\dagger / \alpha_0. \quad (15)$$

In Fig. 4, we graphically solve Eq. (14) for different values of  $\nu$ . In the inset, we plot the solutions,  $z_0^\dagger$ , vs  $\nu \leq 0$ . We find  $z_0^\dagger$  to be a monotonically decreasing function of  $\nu$ . Thus recalling Eq. (2), we conclude that as the potential becomes more repulsive, the transition point  $x_0^\dagger$  is pushed further away from the origin.

From Eq. (14), we see that at the transition point,  $K_{-\nu}(z_0^\dagger)/K_{-1-\nu}(z_0^\dagger) = z_0^\dagger$ , since  $I_{-\nu}(z_0^\dagger) \neq 0$  for  $z_0^\dagger > 0$ . The ratio of the modified Bessel functions of the second kind satisfies the inequality<sup>88</sup>  $K_{-\nu}(y)/K_{-1-\nu}(y) < (-\nu + \sqrt{\nu^2 + y^2})/y$ , leading to an upper bound on  $z_0^\dagger$

$$z_0^\dagger < \sqrt{1 - 2\nu}. \quad (16)$$

In the inset of Fig. 4, we plot this upper bound to show that Eq. (16) provides a simple yet effective way to locate the transition point  $z_0^\dagger$ , bypassing the solution of Eq. (14).

Next, we analyze the behavior of the steady state density in the limit  $x_0 \ll \alpha_0^{-1}$ , i.e., where  $\Pi_r(x)$  is highly asymmetric. To explore this, we set  $x = x_0 + \Delta$  such that  $|\Delta|/x_0 \ll 1$  as before and perform an asymptotic analysis of Eq. (10) in the limit  $x_0 \ll \alpha_0^{-1}$ . The limiting expressions of the modified Bessel functions for small arguments<sup>87</sup> read  $\lim_{y \rightarrow 0} I_{-\nu}(y) \simeq$

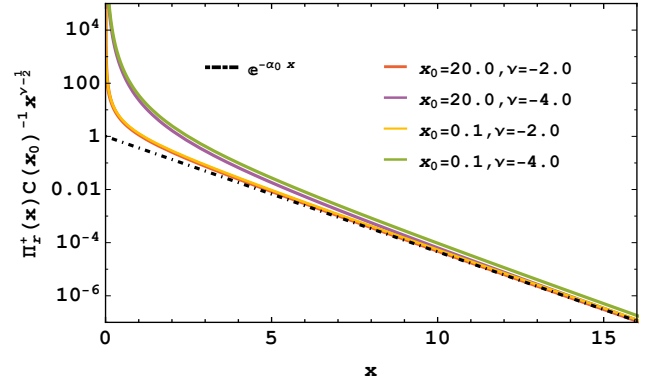


FIG. 6. The scaled steady state distribution  $\Pi_r^+(x)[C(x_0)]^{-1}x^{\nu-\frac{1}{2}}$  for different values of  $\nu$ . Here,  $\Pi_r^+(x)$  is taken from Eq. (10) and  $C(x_0)$  is taken from Eq. (21). The dash-dotted black line shows the limiting expression  $e^{-\alpha_0 x}$  with  $\alpha_0 = 1.0$ .

$2^\nu y^{-\nu}/\Gamma(1-\nu)$  and  $\lim_{y \rightarrow 0} K_{-\nu}(y) \simeq 2^{-1-\nu}y^\nu\Gamma(-\nu)$ , respectively. Utilizing these along with Eq. (10) we obtain

$$\begin{aligned} \Pi_r(x) &= \Pi_r(x_0 + \Delta) \\ &\simeq_{x_0 \ll \alpha_0^{-1}} \begin{cases} -\frac{\alpha_0^2}{2\nu}x & \text{if } \Delta \geq 0, \\ -\frac{\alpha_0^2 x_0^{2\nu}}{2\nu}x^{1-2\nu} & \text{if } \Delta < 0. \end{cases} \end{aligned} \quad (17)$$

In Fig. 5, we plot the steady state distribution  $\Pi_r(x)$  in the limit  $x_0 \ll \alpha_0^{-1}$  for different values of  $\nu$ . Agreement with Eq. (17) is clearly evident.

Finally, we explore how the steady state density decays at large values of  $x$ . We separate two cases; in the limit  $x_0 \gg \alpha_0^{-1}$ , we recall that  $\lim_{y \rightarrow \infty} I_{-\nu}(y) \simeq e^y/\sqrt{2\pi y}$  and  $\lim_{y \rightarrow \infty} K_{-\nu}(y) \simeq e^{-y}\sqrt{\pi/2y}$ , and use Eq. (10) to obtain

$$\Pi_r^+(x) \simeq_{\substack{x_0 \gg \alpha_0^{-1} \\ x \rightarrow \infty}} \frac{\alpha_0}{2} \left(\frac{x}{x_0}\right)^{\frac{1}{2}-\nu} e^{-\alpha_0(x-x_0)}. \quad (18)$$

On the other hand, in the limit  $x_0 \ll \alpha_0^{-1}$ , utilizing the limiting expressions<sup>87</sup>  $\lim_{y \rightarrow 0} I_{-\nu}(y) \simeq 2^\nu y^{-\nu}/\Gamma(1-\nu)$  and  $\lim_{y \rightarrow \infty} K_{-\nu}(y) \simeq e^{-y}\sqrt{\pi/2y}$  together with Eq. (10), we get

$$\Pi_r^+(x) \simeq_{\substack{x_0 \ll \alpha_0^{-1} \\ x \rightarrow \infty}} \frac{\sqrt{\pi}\alpha_0}{\Gamma(1-\nu)} \left[\frac{\alpha_0 x}{2}\right]^{\frac{1}{2}-\nu} e^{-\alpha_0 x}. \quad (19)$$

Comparing Eq. (18) and (19), we see that in the large  $x$  limit

$$\Pi_r^+(x) \simeq_{x \rightarrow \infty} C(x_0) x^{\frac{1}{2}-\nu} e^{-\alpha_0 x}, \quad (20)$$

where the prefactor is given by

$$C(x_0) = \begin{cases} \frac{\alpha_0}{2} x_0^{\nu-\frac{1}{2}} e^{\alpha_0 x_0} & \text{for } x_0 \gg \alpha_0^{-1}, \\ \frac{\sqrt{\pi}\alpha_0}{\Gamma(1-\nu)} \left(\frac{\alpha_0}{2}\right)^{\frac{1}{2}-\nu} & \text{for } x_0 \ll \alpha_0^{-1}. \end{cases} \quad (21)$$

In Fig. 6, we plot the scaled steady state distribution  $\Pi_r^+(x)[C(x_0)]^{-1}x^{\nu-\frac{1}{2}}$  to show that it always converges to the  $\nu$ -independent function  $e^{-\alpha_0 x}$  for large values of  $x$ .

#### IV. FIRST-PASSAGE WITH RESETTING

In the previous section, we explored the non-equilibrium steady state attained for diffusion with resetting in a strongly repulsive logarithmic potential ( $\beta U_0 < -1$ ). In contrast, when the potential is weakly repulsive or attractive ( $\beta U_0 > -1$ ), a steady state is not achieved since the particle will eventually hit the absorbing boundary at the origin<sup>82,84</sup>. Here we explore the effect of stochastic resetting on this first passage process.

Consider a particle that diffuses in a potential  $U(x) = U_0 \log|x|$  with  $\beta U_0 > -1$  and is subject to resetting with a constant rate  $r$ . The conventional way to calculate its first-passage to the absorbing boundary at  $x = 0$  involves the backward Fokker Planck equation approach<sup>30</sup>. In this method, one treats the initial position  $x_0$  as a variable. Hence, we assume that after each resetting event, the particle returns to  $x_r > 0$  (which in principle can be different than its initial position  $x_0 > 0$ ), solve the problem with arbitrary  $x_0$  and  $x_r$  and eventually set  $x_r = x_0$ . Recalling that  $p_r(x, t|x_0)$  is the probability density of finding the particle at position  $x$  at time  $t$ , we see that its backward Fokker Planck equation<sup>29,89</sup> reads

$$\frac{\partial p_r(x, t|x_0)}{\partial t} = -\left(\frac{U_0}{\xi x_0}\right) \frac{\partial p_r(x, t|x_0)}{\partial x_0} + D \frac{\partial^2 p_r(x, t|x_0)}{\partial x_0^2} - r p_r(x, t|x_0) + r p_r(x, t|x_r). \quad (22)$$

The survival probability  $Q_r(t|x_0) := \int_0^\infty p_r(x, t|x_0) dx$ , i.e., the probability that the particle is not absorbed at  $x = 0$  by time  $t$ , then evolves in time following the master equation

$$\frac{\partial Q_r(t|x_0)}{\partial t} = -\left(\frac{U_0}{\xi x_0}\right) \frac{\partial Q_r(t|x_0)}{\partial x_0} + D \frac{\partial^2 Q_r(t|x_0)}{\partial x_0^2} - r Q_r(t|x_0) + r Q_r(t|x_r), \quad (23)$$

where the initial condition is  $Q_r(0|x_0) = 1$  and boundary condition reads  $Q_r(t|0) = 0$ . Eq. (23) is exactly solvable and the solution allows us to directly calculate the moments of the FPT for the process under resetting, bypassing the calculation of  $p_r(x, t|x_0)$ . We present this derivation in Appendix D. In what follows, we obtain the same results in an alternative way, by utilizing the general theory of first passage under resetting<sup>7,10</sup>.

The general theory of first-passage under resetting asserts that the FPT distribution of a process with a constant resetting rate  $r$  can be expressed in terms of the FPT distribution of the process without resetting. Letting  $T$  denote the FPT of some generic process and  $T_r$  its FPT under resetting, one can write<sup>7</sup>

$$\tilde{T}_r(s) = \frac{\tilde{T}(s+r)}{\frac{s}{s+r} + \frac{r}{s+r} \tilde{T}(s+r)}, \quad (24)$$

where  $\tilde{T}(s) := \langle \exp(-sT) \rangle$  and  $\tilde{T}_r(s) := \langle \exp(-sT_r) \rangle$  denote the Laplace transforms of  $T$  and  $T_r$ , respectively. The mean FPT of a generic process under stochastic resetting follows directly from Eq. (24)<sup>7</sup>

$$\langle T_r \rangle = -[d\tilde{T}_r(s)/ds]_{s=0} = \frac{1}{r} \left[ \frac{1 - \tilde{T}(r)}{\tilde{T}(r)} \right]. \quad (25)$$

Eqs. (24) and (25) are completely general. We will now use them to analyze diffusion in weakly repulsive ( $-1 < \beta U_0 < 0$ ) and attractive ( $\beta U_0 > 0$ ) logarithmic potential with stochastic resetting.

Consider first the problem without resetting. The distribution of the first passage time  $T$  to the absorbing boundary at the origin is then given by Eq. (5). Laplace transforming Eq. (5) [Appendix E] we get

$$\tilde{T}(s) = \frac{\left(\sqrt{s x_0^2/D}\right)^\nu K_\nu\left(\sqrt{s x_0^2/D}\right)}{2^{\nu-1} \Gamma(\nu)}. \quad (26)$$

Here again,  $K_\nu(\cdot)$  denotes the modified Bessel function of the second kind and  $\Gamma(\nu)$  denotes the Gamma function. Plugging Eq. (26) into Eq. (24) we obtain

$$\tilde{T}_r(s) = \frac{(s+r) (\alpha x_0)^\nu K_\nu(\alpha x_0)}{s 2^{\nu-1} \Gamma(\nu) + r (\alpha x_0)^\nu K_\nu(\alpha x_0)}, \quad (27)$$

where  $\alpha = \sqrt{(s+r)/D}$ . Eq. (27) provides a closed-form expression for the FPT distribution of the process with resetting in Laplace space. Plugging Eq. (26) into Eq. (25), we obtain the mean FPT to the origin

$$\langle T_r \rangle = \frac{1}{r} \left( \frac{2^{\nu-1} \Gamma(\nu)}{(\alpha_0 x_0)^\nu K_\nu(\alpha_0 x_0)} - 1 \right), \quad (28)$$

where  $\alpha_0 = \sqrt{r/D}$ , as introduced in Sec. III. Note that for  $U_0 = 0$ , i.e., free diffusion,  $\nu = 1/2$  [Eq. (2)]. The mean FPT in this case boils down to  $\langle T_r \rangle = (e^{\sqrt{r x_0^2/D}} - 1)/r$ , which agrees with the result obtained by Evans and Majumdar for free diffusion with stochastic resetting<sup>30</sup>.

The second moment of the FPT can be calculated from Eq. (24) in a similar manner<sup>7</sup>

$$\langle T_r^2 \rangle = [d^2 \tilde{T}_r(s)/ds^2]_{s=0} = 2 \frac{\left[ r \frac{d\tilde{T}(r)}{dr} - \tilde{T}(r) + 1 \right]}{r^2 [\tilde{T}(r)]^2}. \quad (29)$$

Plugging Eq. (26) into Eq. (29), one can calculate  $\langle T_r^2 \rangle$ . The standard deviation of the FPT is then given by

$$\begin{aligned} \sigma(T_r) &:= \sqrt{\langle T_r^2 \rangle - \langle T_r \rangle^2} \\ &= \frac{1}{r} \sqrt{\frac{2^{\nu-1} \Gamma(\nu) [2^{\nu-1} \Gamma(\nu) - (\alpha_0 x_0)^{1+\nu} K_{\nu-1}(\alpha_0 x_0)]}{(\alpha_0 x_0)^{2\nu} [K_\nu(\alpha_0 x_0)]^2} - 1}. \end{aligned} \quad (30)$$

In Fig. 7, we plot the mean and the standard deviation of the FPT vs. the resetting rate  $r$  for different values of  $\beta U_0 \in \{-1, \infty\}$ . We observe four distinct phases shown in panels (a), (b), (c) and (d). These show noticeably different behavior in the limit  $r \rightarrow 0$ . For weakly repulsive ( $-1 < \beta < 0$ ) or weakly attractive ( $0 < \beta U_0 < 1$ ) potential, both the mean and standard deviation of FPT diverge in the absence of resetting, i.e., for  $r = 0$  [panel (a)]. For weak to moderately attractive potential, where  $1 < \beta U_0 < 3$ , the mean FPT in the absence



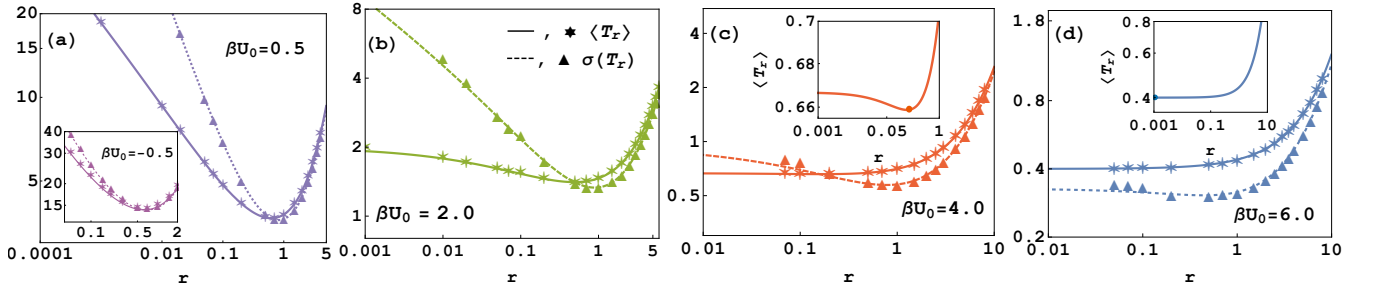


FIG. 7. The mean and the standard deviation of the FPT vs. the resetting rate,  $r$ , for four different phases of diffusion in a logarithmic potential. Lines indicate analytical results [solid lines:  $\langle T_r \rangle$ , dashed lines  $\sigma(T_r)$ ] and symbols show data from simulations [stars:  $\langle T_r \rangle$ , triangles:  $\sigma(T_r)$ ]. Panel (a): For  $-1 < \beta U_0 < 1$ , the mean  $\langle T_r \rangle$  and the standard deviation  $\sigma(T_r)$  of the FPT show a non-monotonic variation with the resetting rate, and both diverge in the limit  $r \rightarrow 0$  (no resetting). Here, we have taken  $\beta U_0 = 0.5$  (main) and  $\beta U_0 = -0.5$  (inset). Panel (b): For  $1 < \beta U_0 < 3$ , the mean and standard deviation of the FPT show a non monotonic variation with the resetting rate. However, while the mean FPT is finite in the limit  $r \rightarrow 0$ , the standard deviation diverges. Here, we have taken  $\beta U_0 = 2$ . Panel (c): For  $3 < \beta U_0 < 5$ , the mean and the standard deviation of FPT still show a non monotonic variation with the resetting rate. Both are finite in the limit  $r \rightarrow 0$ , and  $\sigma(T_{r=0}) > \langle T_{r=0} \rangle$ . Here, we have taken  $\beta U_0 = 4$ . Panel (d): For  $\beta U_0 > 5$ , the mean FPT is monotonically increasing with the resetting rate. Both the mean and standard deviation are finite in the limit  $r \rightarrow 0$ , and  $\sigma(T_{r=0}) < \langle T_{r=0} \rangle$ . The inset of panels (c) and (d) present a zoom in on  $\langle T_r \rangle$  from the corresponding main plots. In all panels we have taken  $x_0 = 2.0$  and  $D = 1.0$ .

of resetting is finite, but the standard deviation at  $r = 0$  diverges [panel (b)]. When the potential is moderately attractive ( $3 < \beta U_0 < 5$ ), both  $\langle T_r \rangle$  and  $\sigma(T_r)$  become finite at  $r = 0$ , with  $\sigma(T_{r=0}) > \langle T_{r=0} \rangle$  [panel (c): main figure]. In this phase, the mean FPT still shows a non-monotonic behavior with the resetting rate [panel (c): inset]. Finally, for strongly attractive potential ( $\beta U_0 > 5$ ), we again find that both  $\langle T_r \rangle$  and  $\sigma(T_r)$  are finite in the absence of resetting, but in contrast to (c) here we have  $\sigma(T_{r=0}) < \langle T_{r=0} \rangle$  [panel (d): main figure]. In this phase,  $\langle T_r \rangle$  monotonically increases with  $r$  [panel (d): inset].

To understand the behavior of the mean and standard deviation of the FPT in the limit  $r \rightarrow 0$ , we use Eq. (5) to calculate the moments of the FPT for the underlying process without resetting. The first moment  $\langle T \rangle := \int_0^\infty t f_T(t) dt$ , i.e., the mean FPT, is found to diverge for weakly repulsive/attractive logarithmic potential, where  $-1 < \beta U_0 < 1$ . Clearly, the standard deviation of the FPT,  $\sigma(T) := \sqrt{\langle T^2 \rangle - \langle T \rangle^2}$ , also diverges in this regime, which supports our observation in panel (a). For  $\beta U_0 > 1$ , using Eq. (5) we obtain the following closed form expression for the mean FPT in the absence of resetting

$$\langle T \rangle = \frac{x_0^2}{2D(\beta U_0 - 1)}, \quad (31)$$

where we recall that  $\beta U_0 = 2v - 1$  [see Eq. (2)]. Eq. (31) shows that  $\langle T \rangle$  is finite for  $\beta U_0 > 1$ . The standard deviation, however, diverges whenever  $\beta U_0 < 3$ . Hence, for  $1 < \beta U_0 < 3$ , the mean FPT is finite but  $\sigma(T)$  diverges [panel (b)].

For  $\beta U_0 > 3$ , the standard deviation of the FPT for the underlying process is finite and given by

$$\sigma(T) = \frac{x_0^2}{\sqrt{2D(\beta U_0 - 1)}\sqrt{\beta U_0 - 3}}. \quad (32)$$

In turn, the theory of first-passage with resetting asserts that the introduction of resetting will result in a decrease of the

mean FPT whenever the ratio between the standard deviation and the mean of the FPT distribution – in the absence of resetting – is larger than unity, and vice versa<sup>7,19</sup>. From Eqs. (31) and (32), we see that here this ratio, commonly known as the coefficient of variation (CV), is given by

$$CV(T) = \frac{\sigma(T)}{\langle T \rangle} = \sqrt{\frac{2}{\beta U_0 - 3}}. \quad (33)$$

From Eq. (33), it is evident that  $CV(T)$  is greater than unity for  $3 < \beta U_0 < 5$ , hence the introduction of resetting lowers the mean FPT in this case. In contrast, for  $\beta U_0 > 5$ ,  $CV(T)$  is less than unity [Eq. (33)]. Therefore, unlike previous cases, here the introduction of resetting hinders first-passage.

In addition to the analytical results of Eqs. (28) and (30), in Fig. 7 we also plot data for  $\langle T_r \rangle$  and  $\sigma(T_r)$  that are obtained by Langevin dynamics simulations. These data are in good agreement with theory. The details of the numerical simulation are given in Appendix C.

In panels (a), (b) and (c), the variation of the mean FPT,  $\langle T_r \rangle$ , with the resetting rate  $r$  is non-monotonic. The minimum of  $\langle T_r \rangle$  in each of these cases is attained at an optimal resetting rate  $r^*$ . In contrast, in panel (d),  $\langle T_r \rangle$  shows a monotonic increase with  $r$ . Moreover, while  $\langle T_r \rangle$  and  $\sigma(T_r)$  intersect in panels (a), (b) and (c), they do not intersect in panel (d). It has recently been shown that for optimally restarted FPT processes the mean is exactly equal to the standard deviation, i.e.,  $\langle T_{r^*} \rangle = \sigma(T_{r^*})$ <sup>7</sup>. Therefore, the intersection points of  $\langle T_r \rangle$  and  $\sigma(T_r)$  in panel (a), (b) and (c) mark the optimal resetting rates. Summarizing, the results above prove that for weakly repulsive and weak to moderately attractive logarithmic potentials, the introduction of resetting accelerates first-passage to the origin, but when the attractive potential is sufficiently strong, resetting cannot expedite the process any more. This clearly indicates a *resetting transition*<sup>46–48</sup> as  $\beta U_0$  grows beyond a critical value. Next, we discuss this transition in terms of the optimal resetting rate  $r^*$ .

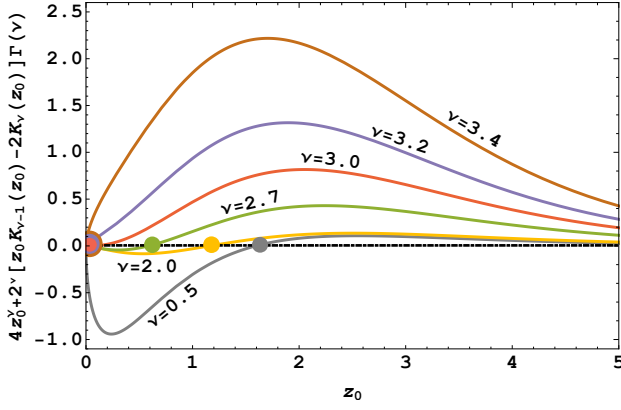


FIG. 8. Graphical solution of Eq. (36) for different values of  $\nu$ . The solutions,  $z_0^*$ , are highlighted by circles.

In order to explicitly calculate the optimal resetting rate, we recall from Sec. III that  $z_0 := \alpha_0 x_0 = \sqrt{r x_0^2 / D}$ . Therefore,

$$r = \frac{D z_0^2}{x_0^2} \quad (34)$$

Plugging Eq. (34) into Eq. (28), we get the mean FPT in terms of  $z_0$  as

$$\langle T_r \rangle = \frac{x_0^2}{D z_0^2} \left[ \frac{2^{\nu-1} \Gamma(\nu)}{z_0^\nu K_\nu(z_0)} - 1 \right]. \quad (35)$$

When the process is reset at an optimal rate,  $r = r^*$ , the mean FPT is minimized hence  $[d\langle T_r \rangle / dr]_{r=r^*} = 0$ . From Eq. (34) we get  $d\langle T_r \rangle / dr \equiv (x_0^2 / 2z_0 D) d\langle T_r \rangle / dz_0$ , which at the optimal resetting rate leads to the following transcendental equation

$$4z_0^\nu + 2^\nu [z_0 K_{\nu-1}(z_0) - 2K_\nu(z_0)] \Gamma(\nu) = 0. \quad (36)$$

In Fig. 8, we graphically solve Eq. (36) for different values of  $\nu$ . The solutions, denoted  $z_0^*$ , can then be utilized to calculate the optimal resetting rates  $r^*$  following Eq. (34). In Fig. 9, we plot these optimal resetting rates vs.  $\beta U_0$  for different values of the initial position  $x_0$ . It is evident from the plot that the point of the resetting transition is always at  $\beta U_0 = 5$ , which does not depend on  $x_0$ . In other words, the introduction of resetting expedites first passage only when the ratio between the strength of the potential and the thermal energy ( $\beta^{-1}$ ) is less than a certain critical value,  $\beta U_0 < 5$ . This critical value is universal in the sense that it is not affected by the initial distance of the particle from the absorbing boundary. This supports the discussion following Eq. (33) which marks the transition at  $CV(T) = 1$ . In the inset of Fig. 9, we plot the optimal resetting rate scaled by the optimal resetting rate for free diffusion to explicitly show that the point of the resetting transition is independent of  $x_0$ .

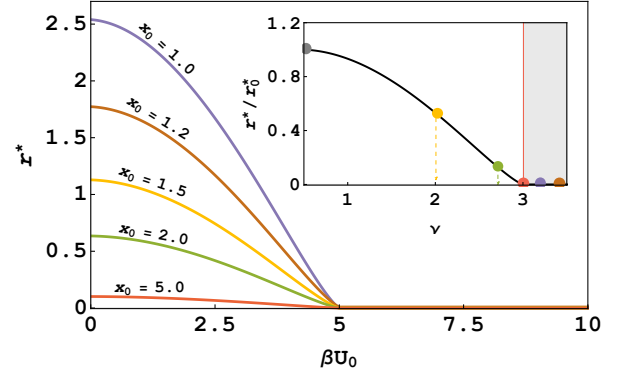


FIG. 9. Main: The optimal resetting rate  $r^*$  vs  $\beta U_0$  for different values of  $x_0$ . The resetting transition is always observed at  $\beta U_0 = 5$ . Beyond this point, the optimal resetting rate is zero, i.e., resetting cannot expedite first passage of the particle to the origin. Inset: The scaled optimal resetting rate  $r^*/r_0^*$  vs the persistent exponent  $\nu = (1 + \beta U_0)/2$ . The resetting transition is observed at  $\nu = 3$ , shown by the vertical orange-red line. The colored circles indicate different values of  $\nu$  from Fig. 8.

## V. CONCLUSIONS

In this work, we presented a comprehensive analysis of the effect of stochastic resetting on diffusion in a logarithmic potential  $U(x) = U_0 \log|x|$ . Here  $U_0$  denotes the strength of the potential which is attractive for  $U_0 > 0$  and repulsive for  $U_0 < 0$ . We found that the effect of resetting on the dynamics of a particle that diffuses in such a logarithmic potential is guided solely by the interplay between this attraction/repulsion energy,  $U_0$ , and the thermal energy  $\beta^{-1}$ . This allows us to construct a phase diagram where transitions between phases occur as the dimensionless parameter  $\beta U_0$  is tuned.

In Fig. 10, we show that the entire range  $\beta U_0 \in \{-\infty, \infty\}$  can be divided into five distinct phases. For  $-\infty < \beta U_0 < -1$ , i.e., for a strongly repulsive potential, the diffusing particle can never reach the origin. In other words, the total probability of finding the particle in the interval  $(0, \infty)$  [assuming that it started its motion at  $x_0 > 0$ ] does not decay with time. The introduction of resetting in this case leads to a steady state which marks phase I in Fig. 10. Detailed analysis of this steady state was provided in Section III.

For  $\beta U_0 > -1$ , i.e., when the potential is either weakly repulsive or attractive, the particle is assured to eventually hit the absorbing boundary at the origin. Based upon the first-passage properties of the system in the limit  $r \rightarrow 0$ , we divide the range  $\beta U_0 \in \{-1, \infty\}$  into four distinct phases. For  $-1 < \beta U_0 < 1$  (weakly repulsive/attractive potential) both the mean and the standard deviation of the FPT diverge in absence of resetting, which marks phase II. For  $1 < \beta U_0 < 3$ ,  $\langle T_{r=0} \rangle$  is finite, but the standard deviation diverges as  $r \rightarrow 0$ , marking phase III. For  $\beta U_0 > 3$ , both the mean and the standard deviation of the FPT in absence of resetting are finite. However, while for  $3 < \beta U_0 < 5$ , the standard deviation is greater than the mean (phase IV), for  $5 < \beta U_0 < \infty$  it is the other way



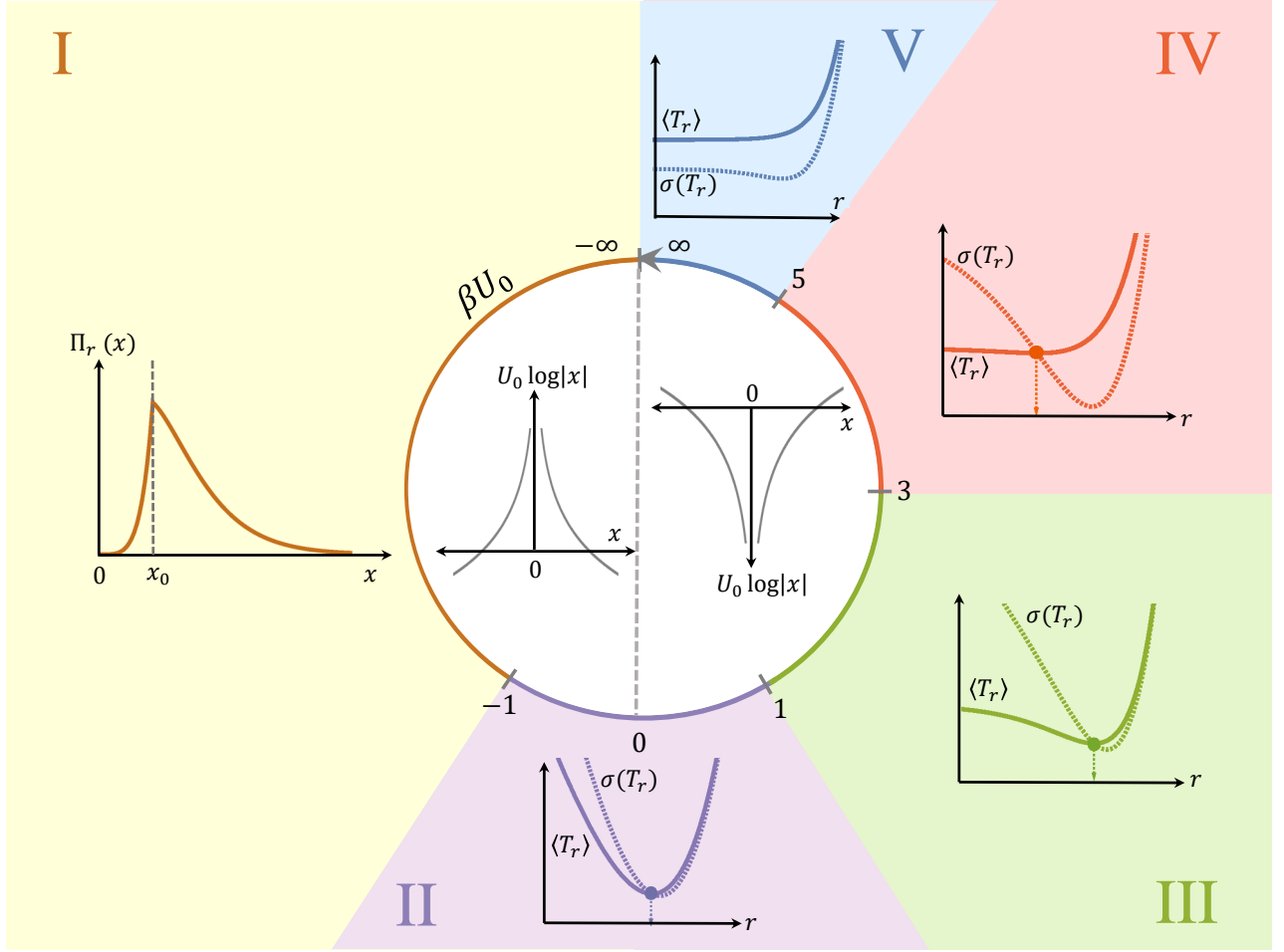


FIG. 10. A phase diagram illustrating the possible effects of stochastic resetting on diffusion in a logarithmic potential  $U(x) = U_0 \log|x|$ . The potential is repulsive for  $U_0 < 0$  and attractive for  $U_0 > 0$ , as shown in the inner circle. Phase transitions occur as  $\beta U_0$ , the ratio between the potential strength and the thermal energy, is tuned. Phase I: A particle, starting from  $x_0$ , will never reach the origin. Resetting the particle to  $x_0$  at a rate  $r$  then results in a nonequilibrium steady state. Phases II-V: A particle, starting from  $x_0$ , will eventually reach the origin. However, in the different phases the behaviour of the mean,  $\langle T_r \rangle$ , and standard deviation,  $\sigma(T_r)$ , of the first passage time is markedly different as elaborately discussed in the main text. In particular, while in phases II-IV the introduction of resetting lowers the mean first passage time, i.e., expedites first passage to the origin, in phase V it is the other way around. The transition between these two markedly different behaviours happens at  $\beta U_0 = 5$  irrespective of the particle's initial position.

around (phase V).

Following the general theory of first-passage with resetting<sup>7</sup>, we can summarize the observations as follows: for phases II, III and IV, i.e., for weakly repulsive or weak to moderately attractive potentials, introduction of resetting accelerates the first-passage of the particle to the origin. In marked contrast, for phase V, i.e., for a strongly attractive potential, resetting delays first-passage to the origin. Moreover, the general theory asserts that at the point of optimal resetting,  $r = r^*$ ,  $\langle T_{r^*} \rangle = \sigma(T_{r^*})$ . Therefore, the fact that the  $\langle T_r \rangle$  and  $\sigma(T_r)$  curves intersect each other for phase II, III and IV, and not for phase V further supports the claim that resetting can expedite first-passage for phases II-IV, but not for phase V.

The effect of resetting on the first-passage of a physical system can, in principle, be inverted by varying the system parameters, e.g. temperature, concentration etc., across some critical point, which gives rise to a “resetting transition”<sup>46–48</sup>.

For diffusion in a potential  $U(x) = U_0 \log|x|$ , we show that the first-passage to the origin can be accelerated by resetting only when the ratio between the repulsion/attraction energy generated from the potential and the thermal energy is less than a certain critical value, viz.,  $\beta U_0 < 5$ . This marks the point of resetting transition at  $\beta U_0 = 5$  (in moving from phase IV to phase V). For the current problem, this transition point is universal in the sense that it is independent of the initial distance of the particle from the absorbing boundary.

## ACKNOWLEDGEMENTS

S. Ray acknowledges support from the Raymond and Beverly Sackler Center for Computational Molecular and Materials Science at Tel Aviv University. S. Reuveni acknowledges support from the Azrieli Foundation, from the Raymond and

Beverly Sackler Center for Computational Molecular and Materials Science at Tel Aviv University, and from the Israel Science Foundation (grant No. 394/19). S. Ray is indebted to Arnab Pal for insightful discussions. The authors thank Arnab Pal and Sarah Kostinski for reading and commenting on early versions of this manuscript.

## APPENDIX A: STEADY STATE DENSITY BY SOLVING EQ. (7)

Eq. (7) in the main text is a second-order, non-linear and inhomogeneous differential equation. Here, we solve Eq. (7) for  $\Pi_r(x)$ , the steady state density for diffusion under resetting in a strongly repulsive logarithmic potential ( $\beta U_0 < -1$ , i.e.,  $\nu < 0$  [see Eq. (2)]). To do that, we perform the following variable transformation

$$\Pi_r(x) \equiv x^\rho y(x). \quad (\text{A.37})$$

Plugging Eq. (A.37) in Eq. (7) and setting  $\alpha_0 = \sqrt{r/D}$  we obtain

$$\frac{d^2 y(x)}{dx^2} + c_1 \left( \frac{1}{x} \right) \frac{dy(x)}{dx} + \left[ \frac{c_2}{x^2} - \alpha_0^2 \right] y(x) = -\alpha_0^2 \frac{\delta(x-x_0)}{x^\rho}, \quad (\text{A.38})$$

where  $c_1 = (2\rho + \beta U_0)$ , and  $c_2 = (\rho - 1)(\rho + \beta U_0)$ . In Eqs. (A.37) and (A.38),  $\rho$  is an arbitrary parameter. Setting  $c_1 = 1$ , we get  $\rho = (1 - \beta U_0)/2 \equiv (1 - \nu)$ , which gives  $c_2 = -[(1 + \beta U_0)/2]^2 \equiv -\nu^2$ . Therefore, Eq. (A.38) reduces to

$$\frac{d^2 y(x)}{dx^2} + \left( \frac{1}{x} \right) \frac{dy(x)}{dx} - \left[ \frac{\nu^2}{x^2} + \alpha_0^2 \right] y(x) = -\alpha_0^2 x^{\nu-1} \delta(x-x_0). \quad (\text{A.39})$$

Eq. (A.39) is an inhomogeneous modified Bessel equation; its general solution is given by

$$y(x) = \begin{cases} A_1 I_{-\nu}(\alpha_0 x) + B_1 K_{-\nu}(\alpha_0 x) & \text{for } x \geq x_0, \\ A_2 I_{-\nu}(\alpha_0 x) + B_2 K_{-\nu}(\alpha_0 x) & \text{for } x < x_0, \end{cases} \quad (\text{A.40})$$

where  $I_{-\nu}(\cdot)$  and  $K_{-\nu}(\cdot)$  are modified Bessel functions of the first and second kind with order  $\nu < 0$ . Since  $\Pi_r(x) = x^{1-\nu} y(x)$ , the general solution of Eq. (7) reads

$$\begin{aligned} \Pi_r^+(x) &= A_1 x^{1-\nu} I_{-\nu}(\alpha_0 x) + B_1 x^{1-\nu} K_{-\nu}(\alpha_0 x) \quad \text{for } x \geq x_0, \\ \Pi_r^-(x) &= A_2 x^{1-\nu} I_{-\nu}(\alpha_0 x) + B_2 x^{1-\nu} K_{-\nu}(\alpha_0 x) \quad \text{for } x < x_0. \end{aligned} \quad (\text{A.41})$$

where  $\Pi_r^+(x)$  and  $\Pi_r^-(x)$  denote the left and right branches of  $\Pi_r(x)$ , respectively. In order to find out the specific solution of Eq. (A.41), we need to calculate the coefficients  $A_1$ ,  $B_1$ ,  $A_2$  and  $B_2$  explicitly, which we accomplish in the following way.

The steady state density  $\Pi_r(x)$  must not diverge at  $x \rightarrow \infty$ , and that sets  $A_1 = 0$ .

In addition,  $\Pi_r(x)$  must be continuous at  $x = x_0$ , i.e.,  $\Pi_r^+(x_0) = \Pi_r^-(x_0)$ . This leads to

$$B_1 = B_2 + A_2 \left[ \frac{I_{-\nu}(\alpha_0 x_0)}{K_{-\nu}(\alpha_0 x_0)} \right]. \quad (\text{A.42})$$

The third condition comes from integrating Eq. (7) over the narrow spatial interval  $[x_0 - \Delta, x_0 + \Delta]$ , where  $|\Delta|/x_0 \ll 1$ , which gives

$$\left[ \frac{d\Pi_r(x)}{dx} \right]_{x_0-\Delta}^{x_0+\Delta} + \beta U_0 \left[ \frac{\Pi_r(x)}{x} \right]_{x_0-\Delta}^{x_0+\Delta} - \alpha_0^2 \int_{x_0-\Delta}^{x_0+\Delta} \Pi_r(x) dx = -\alpha_0^2. \quad (\text{A.43})$$

Here we utilize the identity  $\int_{x_0-\Delta}^{x_0+\Delta} \delta(x-x_0) = 1$ . The condition for continuity at  $x = x_0$  leads to  $[\Pi_r(x)/x]_{x_0-\Delta}^{x_0+\Delta} = 0$  and  $\int_{x_0-\Delta}^{x_0+\Delta} \Pi_r(x) dx = 0$ . Therefore, Eq. (A.43) boils down to

$$\left[ \frac{d\Pi_r(x)}{dx} \right]_{x_0-\Delta}^{x_0+\Delta} \equiv \left[ \frac{d\Pi_r^+(x)}{dx} - \frac{d\Pi_r^-(x)}{dx} \right]_{x=x_0} = -\alpha_0^2. \quad (\text{A.44})$$

Note that Eq. (A.44) is the same as Eq. (13) in the main text, derived in a separate context. Calculating the slopes of  $\Pi_r^\pm(x)$  at  $x = x_0$  from Eq. (A.41) and plugging the results in Eq. (A.44) we get

$$(B_2 - B_1) [K_{-\nu}(\alpha_0 x_0) - \alpha_0 x_0 K_{-\nu-1}(\alpha_0 x_0)] + A_2 [I_{-\nu}(\alpha_0 x_0) + \alpha_0 x_0 I_{-\nu-1}(\alpha_0 x_0)] = \alpha_0^2 x_0^\nu. \quad (\text{A.45})$$

The fourth and final condition comes from the fact that for  $\nu < 0$ , the diffusing particle never reaches the absorbing boundary placed at the origin. Hence,  $\Pi_r(x)$  is normalized to unity, i.e.,  $\int_0^\infty \Pi_r(x) dx \equiv \int_0^{x_0} \Pi_r^-(x) dx + \int_{x_0}^\infty \Pi_r^+(x) dx = 1$ , which leads to

$$B_2 \int_0^{x_0} x^{1-\nu} K_{-\nu}(\alpha_0 x) dx + \frac{x_0^{1-\nu}}{\alpha_0} [A_2 I_{1-\nu}(\alpha_0 x_0) + B_1 K_{1-\nu}(\alpha_0 x_0)] = 1, \quad (\text{A.46})$$

since  $\int_0^{x_0} x^{1-\nu} I_{-\nu}(\alpha_0 x) dx = \alpha_0^{-1} x_0^{1-\nu} I_{1-\nu}(\alpha_0 x_0)$  and  $\int_{x_0}^\infty x^{1-\nu} K_{-\nu}(\alpha_0 x) dx = \alpha_0^{-1} x_0^{1-\nu} K_{1-\nu}(\alpha_0 x_0)$ . Utilizing the general relation  $I_\mu(y) K_{\mu+1}(y) + K_\mu(y) I_{\mu+1}(y) = 1/y$  that is valid for  $\mu \in \mathbb{C}$ , we solve Eqs. (A.42), (A.45), and (A.46) to get the explicit expressions for  $A_2$ ,  $B_1$  and  $B_2$

$$\begin{aligned} B_1 &= \alpha_0^2 x_0^\nu I_{-\nu}(\alpha_0 x_0) \\ A_2 &= \alpha_0^2 x_0^\nu K_{-\nu}(\alpha_0 x_0) \\ B_2 &= 0. \end{aligned} \quad (\text{A.47})$$

Plugging Eq. (A.47) in Eq. (A.41), we get Eq. (10) in the main text.

## APPENDIX B: LAPLACE TRANSFORM OF EQ. (3) FOR STRONGLY REPULSIVE POTENTIAL

Eq. (3) in the main text gives  $p(x, t)$ , the probability density of finding a particle at position  $x$  at time  $t$ , when the particle diffuses in a logarithmic potential. Here, we calculate the Laplace transform of Eq. (3) for  $\beta U_0 < -1$  (or

$v < 0$ ), i.e., when the potential is strongly repulsive. Letting  $\tilde{p}(x, s) := \int_0^\infty e^{-st} p(x, t) dt$  denote the Laplace transform of  $p(x, t)$ , we see that for  $v < 0$

$$\tilde{p}(x, s) = \frac{x}{2D} \left(\frac{x_0}{x}\right)^v \int_0^\infty \frac{e^{-st}}{t} \exp\left(-\frac{x^2 + x_0^2}{4Dt}\right) I_{-v}\left(\frac{xx_0}{2Dt}\right) dt. \quad (\text{B.48})$$

Next, we note the identity<sup>86</sup> that holds for  $\text{Re}(a) \geq \text{Re}(b) > 0$ ,

$$\begin{aligned} & \int_0^\infty e^{-st} \left(\frac{1}{t}\right) \exp\left(-\frac{a+b}{2t}\right) I_\mu\left(\frac{a-b}{2t}\right) dt \\ &= 2K_\mu\left(\sqrt{s}\left(\sqrt{a} + \sqrt{b}\right)\right) I_\mu\left(\sqrt{s}\left(\sqrt{a} - \sqrt{b}\right)\right). \end{aligned} \quad (\text{B.49})$$

Setting  $\mu = -v$  in Eq. (B.49), we compare the integral with that in Eq. (B.48) to identify  $(a+b) \equiv (x^2 + x_0^2)/2D$  and  $(a-b) \equiv (xx_0)/D$ , which gives

$$\sqrt{a} = \frac{(x+x_0)}{2\sqrt{D}} \quad \text{and} \quad \sqrt{b} = \pm \frac{(x-x_0)}{2\sqrt{D}}. \quad (\text{B.50})$$

Therefore, when  $x \geq x_0$ ,  $\sqrt{b} = (x-x_0)/2\sqrt{D}$  and when  $x < x_0$ ,  $\sqrt{b} = (x_0-x)/2\sqrt{D}$ , leading to

$$\begin{aligned} (\sqrt{a} + \sqrt{b}) &= \frac{x}{\sqrt{D}}, \quad (\sqrt{a} - \sqrt{b}) = \frac{x_0}{\sqrt{D}} \quad \text{for } x \geq x_0 \\ (\sqrt{a} + \sqrt{b}) &= \frac{x_0}{\sqrt{D}}, \quad (\sqrt{a} - \sqrt{b}) = \frac{x}{\sqrt{D}} \quad \text{for } x < x_0 \end{aligned} \quad (\text{B.51})$$

Plugging these into Eq. (B.49) and then substituting the integral in Eq. (B.48) accordingly, we get Eq. (9) in the main text by setting  $s = r$ .

## APPENDIX C: DETAILS OF NUMERIC SIMULATION

The Langevin description for a particle diffusing in a potential  $U(x) = U_0 \log|x|$  in the overdamped limit reads

$$\dot{x} = -\frac{U_0}{\zeta x} + \eta(t), \quad (\text{C.52})$$

where  $\zeta$  is the friction coefficient and  $\eta(t)$  denotes a white Gaussian noise with zero mean, i.e.,  $\langle \eta(t) \rangle = 0$  and  $\langle \eta(t)\eta(t') \rangle = 2D\delta(t-t')$ . Here we numerically solve the above stochastic differential equation under resetting with a constant rate  $r$ . This implies that the position of the particle  $x$  is reset to  $x_0$  after random intervals of time taken from an exponential distribution with mean  $r^{-1}$ .

To numerically calculate the steady state density  $\Pi_r(x)$ , we utilize *Heun's method* with step size  $h = 10^{-3}$  to perform the Langevin dynamics simulation and obtain the position  $x$  of the particle in long time limit for  $10^6$  realizations. The steady state distribution is then calculated from the data and compared with the analytical results obtained from Eq. (10) in Fig. 1, which shows that the theoretical results and the simulation data are in striking agreement!

To numerically calculate the mean  $\langle T_r \rangle$  and the standard

deviation  $\sigma(T_r)$  of the FPT to the origin, we perform the Langevin dynamics simulation utilizing *Heun's method* with step size  $h = 10^{-4}$  or  $h = 10^{-6}$ , depending on the system parameters. Smaller step size is necessary to minimize errors in the following cases. For weakly repulsive potential, i.e.,  $-1 < \beta U_0 < 0$ , smaller step size is required to lower down the otherwise high probability of losing the particle downhill when it hits the absorbing boundary at the origin but not immediately detected. For strongly attractive potential,  $\beta U_0 > 5$ , the first passage time  $T_r$  reduces considerably in magnitude, which might lead to large errors if the step size is not sufficiently lower! The simulation is performed for  $10^6$  realizations in each case to calculate the mean and the standard deviation of the FPT; the results when compared with the analytical results from Eq. (28) and Eq. (30), respectively in Fig. 7, show excellent agreement.

## APPENDIX D: FIRST PASSAGE TIME BY SOLVING EQ. (23)

Eq. (23) in the main text is a second order, nonlinear and inhomogeneous partial differential equation. It describes the time evolution of  $Q_r(t|x_0)$ , the survival probability of a particle that diffuses under resetting in a weakly repulsive or attractive logarithmic potential ( $\beta U_0 > -1$ ), in the presence of an absorbing boundary placed at the origin. Here, we solve Eq. (23) in the Laplace space to calculate the mean FPT of the particle to the absorbing boundary. To do that, we set  $\tilde{Q}_r(s|x_0) := \int_0^\infty Q_r(t|x_0)e^{-st} dt$  as the Laplace transform of  $Q_r(t|x_0)$ . Laplace transformation of Eq. (23) then gives

$$\begin{aligned} \frac{d^2 \tilde{Q}_r(s|x_0)}{dx_0^2} - \left(\frac{\beta U_0}{x_0}\right) \frac{d\tilde{Q}_r(s|x_0)}{dx_0} - \left(\frac{s+r}{D}\right) \tilde{Q}_r(s|x_0) = \\ - \frac{1+r\tilde{Q}_r(s|x_r)}{D}, \end{aligned} \quad (\text{D.53})$$

In order to convert Eq. (D.53) to a homogeneous differential equation, we consider a shifted observable  $\tilde{q}(s|x_0) := \tilde{Q}_r(s|x_0) - [(1+r\tilde{Q}_r(s|x_r))/(s+r)]$ . Eq. (D.53) in terms of  $\tilde{q}(s|x_0)$  then reads

$$\frac{d^2 \tilde{q}(s|x_0)}{dx_0^2} - \left(\frac{\beta U_0}{x_0}\right) \frac{d\tilde{q}(s|x_0)}{dx_0} - \left(\frac{s+r}{D}\right) \tilde{q}(s|x_0) = 0. \quad (\text{D.54})$$

Next, we consider another change of variables, viz.,  $\tilde{q}(s|x_0) = x_0^v \tilde{y}(s|x_0)$  with  $v = (1 + \beta U_0)/2$ . Eq. (D.54) then reduces to

$$x_0^2 \frac{d^2 \tilde{y}(s|x_0)}{dx_0^2} + x_0 \frac{d\tilde{y}(s|x_0)}{dx_0} - (\alpha^2 x_0^2 + v^2) \tilde{y}(s|x_0) = 0, \quad (\text{D.55})$$

where  $\alpha = \sqrt{(s+r)/D}$ . Eq. (D.55) is a modified Bessel equation with the general solution

$$\tilde{y}(s|x_0) = A(s)I_v(\alpha x_0) + B(s)K_v(\alpha x_0), \quad (\text{D.56})$$

where  $I_\nu(\alpha x_0)$  and  $K_\nu(\alpha x_0)$  are modified Bessel functions of the first and second kind of order  $\nu > 0$ , respectively. To obtain the specific solution of Eq. (D.55), we need to determine the explicit expressions of  $A(s)$  and  $B(s)$ . We accomplish that in the following way.

We note that in the limit  $x_0 \rightarrow \infty$ , i.e., when the initial position is very far from the absorbing boundary, chances are negligible that the particle is absorbed, and hence the survival probability is unity;  $Q_r(t|x_0)|_{x_0 \rightarrow \infty} = 1$ . That leads to  $\tilde{Q}_r(s|\infty) = 1/s$  and  $\tilde{q}(s|\infty) = 1/s - [(1 + r\tilde{Q}_r(s|x_r))/(s+r)]$  and finally,  $\tilde{y}(s|\infty) = 0$ . Since  $K_\nu(\infty) \rightarrow 0$ , but  $I_\nu(\infty)$  diverges, we set  $A(s) = 0$  to keep things consistent.

To calculate  $B(s)$ , we first assume that the absorbing boundary is kept at  $x = \varepsilon$ . That leads to  $Q_r(t|x_0)|_{x_0=\varepsilon} = 0$ , since the survival probability vanishes if the process is initiated at the absorbing boundary. Therefore,  $\tilde{Q}_r(s|\varepsilon) = 0$  and  $\tilde{q}(s|\varepsilon) = -[(1 + r\tilde{Q}_r(s|x_r))/(s+r)]$ . Thus by definition  $\tilde{y}(s|\varepsilon) = -\varepsilon^{-\nu} [(1 + r\tilde{Q}_r(s|x_r))/(s+r)] \equiv B(s)K_\nu(\alpha\varepsilon)$ . In the limit of  $\varepsilon \rightarrow 0$ , i.e., when the absorbing boundary approaches the origin,  $K_\nu(\alpha\varepsilon) \sim (\alpha\varepsilon)^{-\nu} [2^{\nu-1}\Gamma(\nu)]$ , where  $\Gamma(\nu)$  denotes the gamma function. Comparing, we get  $B(s) = -\alpha^\nu (1 + r\tilde{Q}_r(s|x_r)) / [2^{\nu-1}\Gamma(\nu)(s+r)]$ . Thus the specific solution to Eq. (D.55) reads

$$\tilde{y}(s|x_0) = -\frac{1 + r\tilde{Q}_r(s|x_r)}{2^{\nu-1}\Gamma(\nu)(s+r)} \alpha^\nu K_\nu(\alpha x_0). \quad (\text{D.57})$$

Therefore, the specific solution to Eq. (D.53) is

$$\tilde{Q}_r(s|x_0) = -\left[ \frac{1 + r\tilde{Q}_r(s|x_r)}{2^{\nu-1}\Gamma(\nu)(s+r)} \right] [(\alpha x_0)^\nu K_\nu(\alpha x_0) + 1]. \quad (\text{D.58})$$

We can evaluate  $\tilde{Q}_r(s|x_0)$  in a self consistent manner by putting  $x_r = x_0$  in the above equation, which means that the particle is taken back to the initial position after resetting. After simplification, that reads

$$\tilde{Q}_r(s|x_0) = \frac{2^{\nu-1}\Gamma(\nu) - (\alpha x_0)^\nu K_\nu(\alpha x_0)}{s 2^{\nu-1}\Gamma(\nu) + r (\alpha x_0)^\nu K_\nu(\alpha x_0)}. \quad (\text{D.59})$$

Eq. (D.59) allows us to compute the first passage time (FPT) of the particle to the absorbing boundary. Letting  $T_r$  denote this FPT, we recall that the probability density function of this random variable is given by  $-dQ_r(t|x_0)/dt$ <sup>89</sup>. This allows us to calculate any moment of  $T_r$  from  $\tilde{Q}(s|x_0)$ . In particular, the first moment or the mean FPT is given by  $\langle T_r \rangle = -\int_0^\infty t(dQ_r(t|x_0)/dt)dt = [\tilde{Q}_r(s|x_0)]_{s=0}$ . We see that for  $s = 0$ ,  $\alpha = \sqrt{r/D} \equiv \alpha_0$ . Setting  $s = 0$  and  $\alpha = \alpha_0$  in Eq. (D.59), we obtain Eq. (28).

## APPENDIX E: LAPLACE TRANSFORM OF EQ. (5)

Eq. (5) presents  $f_T(t)$ , the first passage time distribution to the origin for a particle that diffuses in a weakly repulsive or attractive logarithmic potential with  $\beta U_0 > -1$ . Letting

$\tilde{T}(s) := \int_0^\infty e^{-st} f_T(t) dt$  denote the Laplace transform of  $f_T(t)$ , from Eq. (5) we get

$$\tilde{T}(s) = \frac{1}{\Gamma(\nu)} \left( \frac{x_0^2}{4D} \right)^\nu \int_0^\infty t^{-(\nu+1)} \exp\left(-st - \frac{x_0^2}{4Dt}\right) dt \quad (\text{E.60})$$

Next, we note the following relation<sup>90</sup>

$$\int_0^\infty x^{\gamma-1} \exp\left(-x - \frac{\mu^2}{4x}\right) dx = 2 \left( \frac{\mu}{2} \right)^\gamma K_{-\gamma}(\mu), \quad (\text{E.61})$$

which holds for  $|\arg(\mu)| < \pi/2$  and  $\text{Re}(\mu^2) > 0$ . Considering a scaling  $t \rightarrow st$  in Eq. (E.60), we compare the integrals in Eqs. (E.60) and (E.61) to identify  $\gamma = -\nu$  and  $\mu = \sqrt{s x_0^2/D}$ . Evaluating the integral in Eq. (E.61) with these and plugging the result into Eq. (E.60), we obtain Eq. (26) in the main text.

## REFERENCES:

- <sup>1</sup>M. Luby, A. Sinclair, and D. Zuckerman, *Optimal speedup of Las Vegas algorithms*, *Inf. Process Lett.* **47**, 173, (1993).
- <sup>2</sup>C. P. Gomes, B. Selman, and H. Kautz, *Boosting combinatorial search through randomization*, *AAAI/IAAI* **98**, 431, (1998).
- <sup>3</sup>A. Montanari and R. Zecchina, *Optimizing searches via rare events*, *Phys. Rev. Lett.* **88**, 178701, (2002).
- <sup>4</sup>D. S. Steiger, T. F. Rønnow, and M. Troyer, *Heavy tails in the distribution of time to solution for classical and quantum annealing*, *Phys. Rev. Lett.* **115**, 230501 (2015).
- <sup>5</sup>Ł. Kuśmierz, S. N. Majumdar, S. Sabhapandit, and G. Schehr, *First order transition for the optimal search time of Lévy flights with resetting*, *Phys. Rev. Lett.* **113**, 220602, (2014).
- <sup>6</sup>Ł. Kuśmierz, and E. Gudowska-Nowak, *Optimal first-arrival times in Lévy flights with resetting*, *Phys. Rev. E* **92**, 052127, (2015).
- <sup>7</sup>S. Reuveni, *Optimal stochastic restart renders fluctuations in first passage times universal*, *Phys. Rev. Lett.* **116**, 170601 (2016).
- <sup>8</sup>A. Pal, A. Kundu, and M. R. Evans, *Diffusion under time-dependent resetting*, *J. Phys. A: Math. Theor.* **49** 225001, (2016).
- <sup>9</sup>U. Bhat, C. De Bacco, and S. Redner, *Stochastic search with Poisson and deterministic resetting* *J. Stat. Mech.* **2016**, 083401, (2016).
- <sup>10</sup>A. Pal, and S. Reuveni, *First Passage under Restart*, *Phys. Rev. Lett.* **118**, 030603, (2017).
- <sup>11</sup>A. Chechkin, and I. M. Sokolov, *Random search with resetting: a unified renewal approach*, *Phys. Rev. Lett.* **121**, 050601, (2018).
- <sup>12</sup>M. R. Evans, and S. N. Majumdar, *Effects of refractory period on stochastic resetting*, *J. Phys. A: Math. Theor.* **52**, 01LT01, (2018).
- <sup>13</sup>I. Eliazar, *Branching search*, *EPL* **120**, 60008, (2018).
- <sup>14</sup>A. Pal, I. Eliazar, and S. Reuveni, *First passage under restart with branching*, *Phys. Rev. Lett.* **122**, 020602, (2019).
- <sup>15</sup>G. M. Viswanathan, M. G. E. da Luz, E. P. Raposo, and H. E. Stanley, *The Physics of Foraging: An Introduction to Random Searches and Biological Encounters*, Cambridge U. Press, New York (2011).
- <sup>16</sup>A. Pal, Ł. Kuśmierz, and S. Reuveni, *Home-range search provides advantage under high uncertainty*, *arXiv:1906.06987*, (2019).
- <sup>17</sup>P. Visco, R. J. Allen, S. N. Majumdar, and M. R. Evans, *Switching and growth for microbial populations in catastrophic responsive environments*, *Biophys. J.* **98**, 1099 (2010).
- <sup>18</sup>D. Sornette, *Critical market crashes*, *Phys. Rep.* **378**, 1, (2003).
- <sup>19</sup>S. Reuveni, M. Urbakh, and J. Klafter, *Role of substrate unbinding in Michaelis-Menten enzymatic reactions*, *Proc. Natl. Acad. Sci. U. S. A.* **111**, 4391 (2014).
- <sup>20</sup>T. Rotbart, S. Reuveni, and M. Urbakh, *Michaelis-Menten reaction scheme as a unified approach towards the optimal restart problem*, *Phys. Rev. E* **92**, 060101 (2015).

- <sup>21</sup>A. M. Berezhkovskii, A. Szabo, T. Rotbart, M. Urbakh, and A. B. Kolomeisky, *Dependence of the Enzymatic Velocity on the Substrate Dissociation Rate*, *J. Phys. Chem. B* **121**, 3437 (2016).
- <sup>22</sup>T. Robin, S. Reuveni, and M. Urbakh, *Single-molecule theory of enzymatic inhibition*, *Nat. Commun.* **9**, 779 (2018).
- <sup>23</sup>F. Wong, A. Dutta, D. Chowdhury, and J. Gunawardena, *Structural conditions on complex networks for the Michaelis-Menten input/output response*, *Proc. Natl. Acad. Sci. USA* **115**, 9738, (2018).
- <sup>24</sup>É. Roldán, A. Lisica, D. Sánchez-Taltavull, and S. W. Grill, *Stochastic resetting in backtrack recovery by RNA polymerases*, *Phys. Rev. E* **93**, 062411 (2016).
- <sup>25</sup>I. Eliazar, T. Koren, and J. Klafter, *Searching circular DNA strands*, *J. Phys.: Condens. Matter* **19**, 065140 (2007).
- <sup>26</sup>I. Eliazar, T. Koren, and J. Klafter, 2008. *Parallel search of long circular strands: Modeling, analysis, and optimization*, *J. Phys. Chem. B* **112**, 5905, (2008).
- <sup>27</sup>S. Budnar, K. B. Husain, G. A. Gomez, M. Naghibosadat, A. Varma, S. Verma, N. A. Hamilton, R. G. Morris, and A. S. Yap, *Anillin promotes cell contractility by cyclic resetting of RhoA residence kinetics*, *Dev. Cell.* **49**, 894 (2019).
- <sup>28</sup>Y. E. Kim, M. S. Hipp, A. Bracher, M. Hayer-Hartl, and F. U. Hartl, *Molecular chaperone functions in protein folding and proteostasis*, *Annu. Rev. Biochem.* **82**, 323 (2013).
- <sup>29</sup>M. R. Evans, S. N. Majumdar, and G. Schehr, *Stochastic resetting and applications*, *J. Phys. A: Math. Theor.* in press, doi:10.1088/1751-8121/ab7cfe, (2020).
- <sup>30</sup>M. R. Evans, and S. N. Majumdar, *Diffusion with stochastic resetting*, *Phys. Rev. Lett.* **106**, 160601 (2011).
- <sup>31</sup>M. R. Evans, and S. N. Majumdar, *Diffusion with optimal resetting*, *J. Physics A: Math. Theor.* **44**, 435001 (2011).
- <sup>32</sup>M. R. Evans, S. N. Majumdar, and K. Mallick, *Optimal diffusive search: nonequilibrium resetting versus equilibrium dynamics*, *J. Physics A: Math. Theor.* **46**, 185001 (2013).
- <sup>33</sup>M. R. Evans, and S. N. Majumdar, *Diffusion with resetting in arbitrary spatial dimension*, *J. Physics A: Math. Theor.* **47**, 285001 (2014).
- <sup>34</sup>C. Christou, and A. Schadschneider, *Diffusion with resetting in bounded domains*, *J. Physics A: Math. Theor.* **48**, 285003 (2015).
- <sup>35</sup>A. Pal, A. Kundu, and M. R. Evans, *Diffusion under time-dependent resetting*, *J. Physics A: Math. Theor.* **49**, 225001 (2016).
- <sup>36</sup>A. Nagar, and S. Gupta, *Diffusion with stochastic resetting at power-law times*, *Phys. Rev. E* **93**, 060102 (2016).
- <sup>37</sup>S. Eule, and J. J. Metzger, *Non-equilibrium steady states of stochastic processes with intermittent resetting*, *New J. Phys.* **18**, 033006 (2016).
- <sup>38</sup>A. Pal, and V. V. Prasad, *First passage under stochastic resetting in an interval*, *Phys. Rev. E*, **99**, 032123 (2019).
- <sup>39</sup>A. Pal, R. Chatterjee, S. Reuveni, and A. Kundu, *Local time of diffusion with stochastic resetting*, *J. Physics A: Math. Theor.* **52**, 264002 (2019).
- <sup>40</sup>A. Pal, Ł. Kusmierz, and S. Reuveni, *Time-dependent density of diffusion with stochastic resetting is invariant to return speed*, *Phys. Rev. E* **100**, 040101, (2019).
- <sup>41</sup>A. Pal, Ł. Kusmierz, and S. Reuveni, *Invariants of motion with stochastic resetting and space-time coupled returns*, *New J. Phys.* **21**, 113024, (2019).
- <sup>42</sup>O. Tal-Friedman, A. Pal, A. Sekhon, S. Reuveni, and Y. Roichman, *Experimental realization of diffusion with stochastic resetting*, arXiv:2003.03096, (2020).
- <sup>43</sup>S. Redner, *A guide to first-passage processes*, Cambridge University Press, (2001).
- <sup>44</sup>A. J. Bray, S. N. Majumdar, and G. Schehr, *Persistence and first-passage properties in nonequilibrium systems*, *Adv. Phys.* **62**, 225, (2013).
- <sup>45</sup>A. Pal, *Diffusion in a potential landscape with stochastic resetting* *Phys. Rev. E* **91**, 012113 (2015).
- <sup>46</sup>A. Pal and V. V. Prasad, *Landau theory of restart transitions*, *Phys. Rev. Research* **1**, 032001 (2019).
- <sup>47</sup>S. Ray, D. Mondal, and S. Reuveni, *Péclet number governs transition to acceleratory restart in drift-diffusion*, *J. Phys. A: Math. Theor.* **52**, 255002 (2019).
- <sup>48</sup>S. Ahmad, I. Nayak, A. Bansal, A. Nandi, and D. Das, *First passage of a particle in a potential under stochastic resetting: a vanishing transition of optimal resetting rate*, *Phys. Rev. E* **99**, 022130 (2019).
- <sup>49</sup>É. Roldán and S. Gupta, *Path-integral formalism for stochastic resetting: Exactly solved examples and shortcuts to confinement*, *Phys. Rev. E* **96**, 022130 (2017).
- <sup>50</sup>D. Gupta, C. A. Plata, and A. Pal, *Work Fluctuations and Jarzynski Equality in Stochastic Resetting*, *Phys. Rev. Lett.* **124**, 110608 (2020).
- <sup>51</sup>D. Poland and H. A. Scheraga, *Phase Transitions in One Dimension and the Helix-Coil Transition in Polyamino Acids*, *J. Chem. Phys.* **45**, 1456 (1966).
- <sup>52</sup>D. Poland and H. A. Scheraga, *Occurrence of a Phase Transition in Nucleic Acid Models*, *J. Chem. Phys.* **45**, 1464 (1966).
- <sup>53</sup>A. Bar, Y. Kafri, and D. Mukamel, *Loop Dynamics in DNA Denaturation*, *Phys. Rev. Lett.* **98**, 038103 (2007).
- <sup>54</sup>C. Fogedby and R. Metzler, *DNA Bubble Dynamics as a Quantum Coulomb Problem*, *Phys. Rev. Lett.* **98**, 070601 (2007).
- <sup>55</sup>A. Bar, Y. Kafri, and D. Mukamel, *Dynamics of DNA melting*, *J. Phys.: Condens. Matter* **21**, 034110 (2009).
- <sup>56</sup>V. Kaiser and T. Novotný, *Loop exponent in DNA bubble dynamics*, *J. Phys. A: Math. Theor.* **47**, 315003 (2014).
- <sup>57</sup>D. A. Kessler and E. Barkai, *Infinite Covariant Density for Diffusion in Logarithmic Potentials and Optical Lattices*, *Phys. Rev. Lett.* **105**, 120602 (2010).
- <sup>58</sup>A. Dechant, E. Lutz, D. A. Kessler, and E. Barkai, *Fluctuations of Time Averages for Langevin Dynamics in a Binding Force Field*, *Phys. Rev. Lett.* **107**, 240603 (2011).
- <sup>59</sup>A. Dechant, E. Lutz, E. Barkai, and D. A. Kessler, *Solution of the Fokker-Planck Equation with a Logarithmic Potential*, *J. stat. Phys.* **145**, 1524 (2011).
- <sup>60</sup>A. Dechant, E. Lutz, D. A. Kessler, and E. Barkai, *Superaging correlation function and ergodicity breaking for Brownian motion in logarithmic potentials*, *Phys. Rev. E* **85**, 051124 (2012).
- <sup>61</sup>D. A. Kessler and E. Barkai, *Theory of Fractional Lévy Kinetics for Cold Atoms Diffusing in Optical Lattices*, *Phys. Rev. Lett.* **108**, 230602 (2012).
- <sup>62</sup>E. Lutz and F. Renzoni, *Beyond Boltzmann-Gibbs statistical mechanics in optical lattices*, *Nat. Phys.* **9**, 615 (2013).
- <sup>63</sup>N. Leibovich and E. Barkai, *Aging Wiener-Khinchin Theorem*, *Phys. Rev. Lett.* **115**, 080602 (2015).
- <sup>64</sup>N. Leibovich, A. Dechant, E. Lutz, and E. Barkai, *Aging Wiener-Khinchin Theorem and critical exponents of  $1/f^\beta$  noise*, *Phys. Rev. E* **94**, 052130 (2016).
- <sup>65</sup>R. Zwanzig, *Diffusion Past an Entropy Barrier*, *J. Phys. Chem.* **96**, 3926 (1992).
- <sup>66</sup>D. Reguera and J. M. Rubí, *Kinetic equations for diffusion in the presence of entropic barriers*, *Phys. Rev. E* **64**, 061106 (2001).
- <sup>67</sup>M. Muthukumar, *Polymer escape through a nanopore*, *J. Phys. Chem.* **118**, 5174 (2003).
- <sup>68</sup>D. Mondal, M. Das, and D. S. Ray, *Entropic resonant activation*, *J. Phys. Chem.* **132**, 224102 (2010).
- <sup>69</sup>D. Mondal, M. Das, and D. S. Ray, *Entropic noise-induced nonequilibrium transition*, *J. Phys. Chem.* **133**, 204102 (2010).
- <sup>70</sup>D. Mondal, *Enhancement of entropic transport by intermediates*, *Phys. Rev. E* **84**, 011149 (2011).
- <sup>71</sup>D. Mondal, and D. S. Ray, *Asymmetric stochastic localization in geometry controlled kinetics*, *J. Phys. Chem.* **135**, 194111 (2011).
- <sup>72</sup>F. J. Dyson, *A Brownian-Motion Model for the Eigenvalues of a Random Matrix*, *J. Math. Phys.* **3**, 1191 (1962).
- <sup>73</sup>H. Spohn, *Tracer dynamics in Dyson's model of interacting Brownian particles*, *J. Stat. Phys.* **47**, 669 (1987).
- <sup>74</sup>F. Bouchet and T. Dauxois, *Prediction of anomalous diffusion and algebraic relaxations for long-range interacting systems, using classical statistical mechanics*, *Phys. Rev. E* **72**, 045103 (1992).
- <sup>75</sup>P. H. Chavanis, C. Rosier, and C. Sire, *Thermodynamics of self-gravitating systems* *Phys. Rev. E* **66**, 036105 (2002).
- <sup>76</sup>C. Sire and P. H. Chavanis, *Thermodynamics and collapse of self-gravitating Brownian particles in D dimensions*, *Phys. Rev. E* **66**, 046133 (2002).
- <sup>77</sup>S. Manning, *Limiting Laws and Counterion Condensation in Polyelectrolyte Solutions I. Colligative Properties*, *J. Chem. Phys.* **51**, 924 (1969).
- <sup>78</sup>D. Mondal and M. Muthukumar *Ratchet rectification effect on the translocation of a flexible polyelectrolyte chain*, *J. Chem. Phys.* **145**, 084906 (2016).

- <sup>79</sup>E. Levine, D. Mukamel, and G. M. Schütz, *Zero-Range Process with Open Boundaries*, *EPL* **47**, 565 (2005).
- <sup>80</sup>O. Hirschberg, D. Mukamel and G. M. Schütz, *Approach to equilibrium of diffusion in a logarithmic potential* *Phys. Rev. E* **84**, 041111 (2011).
- <sup>81</sup>O. Hirschberg, D. Mukamel and G. M. Schütz, *Diffusion in a logarithmic potential: scaling and selection in the approach to equilibrium* *J. Stat. Mech.* **2012**, 02001 (2012).
- <sup>82</sup>A. J. Bray, *Random walks in logarithmic and power-law potentials, nonuniversal persistence, and vortex dynamics in the two-dimensional XY model*, *Phys. Rev. E* **62**, 103 (2000).
- <sup>83</sup>E. Martin, U. Behn and G. Germano, *First-passage and first-exit times of a Bessel-like stochastic process* *Phys. Rev. E* **83**, 051115 (2011).
- <sup>84</sup>A. Ryabov, E. Berestneva, and V. Holubec, *Brownian motion in time-dependent logarithmic potential: Exact results for dynamics and first-passage properties*, *J. Chem. Phys.* **143**, 114117 (2015).
- <sup>85</sup>D. R. Cox, and H.D. Miller, *The Theory of Stochastic Processes*, *CRC Press*, [See Eq. (74) in Chapter 5] (2001).
- <sup>86</sup>A. Erdélyi, W. Magnus, F. Oberhettinger and F. G. Tricomi, *Tables of Integral Transforms*, Volume I, California Institute of Technology, Bateman Manuscript Project (Based, in part, on notes left by Late Prof. Harry Bateman), McGrawHill Book Comp., Inc. (1954). [See Eq. (4) in page 200].
- <sup>87</sup>Digital Library of Mathematical Functions, National Institute of Standards and Technology (NIST), U.S. Department of Commerce, <https://dlmf.nist.gov/>.
- <sup>88</sup>A. Laforgia and P. Natalini, *Some Inequalities for Modified Bessel Functions*, *J. Inequal. Appl.* **2010**, 253035 (2010).
- <sup>89</sup>C. W. Gardiner, *Handbook of Stochastic Methods for Physics, Chemistry and the Natural Sciences*, Springer-Verlag., (2003).
- <sup>90</sup>I. S. Gradshteyn, I. M. Ryzhik, D. Zwillinger and V. Moll, *Table of integrals, series, and products*, *Academic Press, Elsevier Inc.*, 8th Edition, (2014). [See Eq. 12 of Section 3.474 in page 371].